Universidad Carlos III de Madrid

Escuela Politécnica Superior de Leganés

BACHELOR THESIS

Javier Gómez del Pulgar Vázquez

One Dimensional Particle Mover and PIC Code applied to Electron Cyclotron Resonance Thruster

Bioengineering and Aerospace Engineering Department

Supervisor of the degree thesis: Álvaro Sánchez Villar

Study programme: Aeronautics

Specialization: Aerospace Propulsion

Leganés 2018

Acknowledments

En esta sección quería agradecer a todos aquellos que me han apoyado durante todos estos años de carrera y que han hecho posible que sea capaz de entregar este proyecto. Quería agradecer a mi familia y amigos por el constante apoyo que me han dado durante prácticamente toda mi vida. Sin ellos esto no sería posible.

Especial atención a mi tutor Álvaro Sánchez, cuyo apoyo ha sido constante a lo largo de todo el proyecto. Me ha sabido guiar y he aprendido mucho con él de esta experiencia.

Abstract

This project aims to describe a simplified model of the plasma-wave interaction that occurs inside the chamber of a typical Electron Cyclotron Resonance Thruster. As its name suggests, ECR thrusters are based on the resonance of the electron with a given polarized electromagnetic wave, the so-called, Right Hand Polarized wave. This is a problem known since the early 60's, however, due to technical reasons, the reseaech was abandoned. Recently, it has been resumed by research institutes as Onera or universities as UC3M, in the context of MINOTOR H2020 project.

The project is devoted in the construction of a code that allows to study the interaction of a given population of electrons with a prescribed RHP wave, which it is assumed to be constant despite the changes on plasma properties. Different parameters will be studied and followed along time to check how the resonance affects the initial electron parameters.

The second second part of this project is the introduction of numerical computation in plasma physics with the add-on of a PIC code, where particle properties are weighted inside a grid mesh.

Keywords: Electron Cyclotron Resonance, electric propulsion, electric thrusters, Right Hand Polarized.

Contents

List of Figures

List of Tables

Motivation, socio-economic impact and research objectives

1.1 Motivation

The motivation behind the development of this project lies in the fact that the Electron Cyclotron Resonance thruster is at its early beginnings of development. In that sense, a complete understanding of the behaviour of the plasma physics that is presence on this thruster is yet to be fully understand. I In that sense, there is an international effort to develop a close model of the engine, optimizing it for future space missions, taking advantages of the features that this thruster can offer. One of the most recognized project developed to this effort, is the MINOTOR H2020 [6], an international European-based team whose objective is to prove the feasibility of the ECR thruster. This project, is divided in different researches group that are scattered around Europe. For instance, a team in France is devoted to the creation of a high efficiency microwave generator, while a different group based in Germany focus their efforts into testing different power levels, in order to determine which is the optimize power input.

One of the main problems that are yet to be understood is the deposition of power from the electromagnetic wave to the electron population. In that sense, this project aims to describe the physics behind that power deposition and discover the parameters affecting its efficiency. One of the main drivers of this investigation for the MINOTOR project is the *Universidad Carlos III de Madrid*, whose task is the development of a numerical model that simulates the conditions of the chamber inside a ECR thruster.

1.2 Socio-economical impact and regulatory framework

Space budget is currently on an increasing trend in terms of founding and budget [7]. For instance, the budget destined to the NASA research and growth has increased

from $ 13.6 billion dollars in the year 1998 to more than $ 20 billion in the current year. Although the current trend is clear, more funding, the amount is far from what other departments of USA receives, being more than $ 80 billion what the Veteran Administration receives or, looking at the Defense Department, the astronomical digit of $ 600 billion. Nevertheless, investing in NASA or in space research in general seems promising, as each dollar invested generates profit. Bearing in mind that the space industry is supported by many other industries and departments (Federal Aviation Administration, Defense Department among others), it seems reasonable that the previously increasing trend not only will be continuously growing, but accelerating.

Alongside public investing in NASA, there exists a program destined to private companies to encourage space missions, especially low-Earth missions. Companies such as SpaceX, Boeing or Axiom Space are working to bring closely space investigation.

Considering the second major space agent, ESA, its budget for the current year has an approximate value of €5.6 billion, which is divided into different areas of investigation as represented.

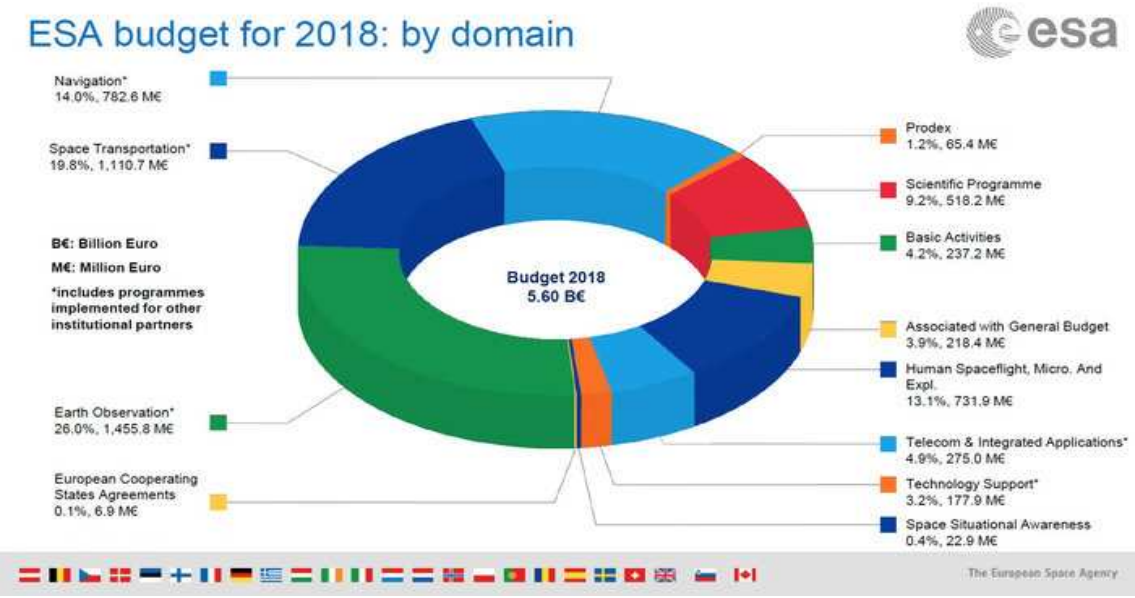

Figure 1.1: ESA budget for 2018 [1]

The money that is invested in ESA activities comes from all the members of the European Union according to their Gross Domestic Product (GPD). The areas of research in which the ESA activities are divides can be joined into two groups, mandatory activities and optional activities. Mandatory activities are the main core of ESA, involving technological research, training programmes or future projects. All members must contribute to this mandatory departments. Optional activities, which involves telecommunication research or the International Space Station only receives funds for the countries that are interested in those programmes. As an extra, ESA also accepts funds from private investments.

As the space industry acquires more and more relevance in the global market and on future projects, more money and funds will be deposited into the investigation of new technologies. Among those technologies, electric propulsion is seen as the future of propulsion due to its cost savings and efficiencies. Even though the current state of electric propulsion is far from being completed, the really good performance of in-mission electric engines alongside the promising results of new propulsive projects, requires following the investigation trend.

However, investing in the space industry and propulsion systems is not only beneficial to that particular industry. As previously stated, the inversion in such programmes has an additional effect on improving everyone's life. As an example, satellite communication or the Global Navigation Satellite System (GNSS).

Focusing on the Electron Cyclotron Resonance thruster, there is a current trend in investing in electric propulsion. The cost-savings related to the usage of this kind of engines versus the conventional liquid propellant engines make investing in this type of technology a good opportunity for future missions as new spacecraft will be smaller or will have a capacity for greater payloads. In addition to that, ECR thrusters are part of the electrodeleess family along with the Helicon Plasma Thuster. That implies that, although currently not so efficient as Gridded Ion thrusters or Helicon Plasma thrusters, the advantages of this new engines (low power input, longer lifetime, magnetic thrust vectoring...) will make the difference in the near future.

Regarding the regulatory framework of the current space industry, current laws are based on the 1967 Outer Space Treaty [8]. On its most basic description, this treaty explains that each country is responsible for its operations and the potential damage that those countries may cause.

Roughly speaking any country which has signed this document has some obligations in terms of space missions. Firstly, its investigations, although carried under its own sovereignty, must be focused on the global interest, independent on the different socio-economical characteristics of the country itself. A country member is enforced to provide help if needed. For instance, in the case of astronaut rescue and his return to the Earth, should be the case. Finally as a main issue, any activity that may cause potential danger is, in a large degree, monitored by the United Nations. This fact includes the launching of nuclear weapons or nuclear power sources.

The 1967 Outer Space Treaty has been revised for the following years, adding some new information regarding space exploration and activities on celestial bodies. As an example, the regulation of the Moon activities. This treaty enforces member countries to follow the international law while the exploration and use of the Moon, which states that it is only subjected to peacefully and scientific researches. Any objective out of this scope is considered as a violation of the agreement.

As a brief summary of the Outer Space Treaty, each country is able to launch its missions to the space, becoming responsible of what they send and what they may leave there.

1.3 Objectives and description of this work

This project has the objective of developing a simplified analysis of the resonance behaviour between an electron distribution and a prescribed RHP microwave profile. Regarding the fulfillment of this project, a custom code has been developed for this purpose in which a particle mover has been created alongside some of the PIC properties to mesh how the electron distribution evolves.

Regarding the particle mover, a standard set of differential equations are derived to study how the velocities evolve in time according to the existing electromagnetic fields. During the developing of this equations, the condition required for resonance will be explained. Regarding the involving of the PIC code, the weighting mechanism has been included in the overall of the code, so that at each time step, information about plasma densities will be evaluated.

State of the art of electric propulsion

Electric thrusters are a reality since the beginnings of the nineteenth century, where the first concepts and models were studied. However, it was not until the late 60's and early 70's when scientists all around the world started to include those previous studies made by its predecessors on new satellite propulsion systems. Currently, hundreds of satellites orbiting the Earth use electric thrusters for orbital station-keeping or even for orbital changing manoeuvres.

Electric propulsion (EP) is continuously being investigated and revised to overcome some major difficulties associated with this type of propulsion in which we can find:

- Lifetime. Due to the rapid erosion of some of the components of current engines, this kind of engines are not supported for long term missions (~ 5 years).

- Limited amount of thrust. These engines provide thrust by expelling ions at high velocity. Nevertheless, although being a continuous thrust, the low mass that is expelled does not provide with great accelerations. This leads to increased mission duration.

- Limited electric power on board. Studies have shown that great propulsive efficiencies are reached by supplying large amount of power to the system. Current on-board power units provide with a fraction of the required for competitive efficiencies.

Despite its limitations, EP offers great advantages compared to a traditional liquid or hybrid propulsion systems, in which an oxidizer and a reactant react in a combustion chamber generating a gas that it is expelled to create thrust. The main drawback of these rockets is the amount of fuel and, consequently, mass that needs to be transported inside tanks. EP reduces considerably the amount of fuel needed due to its higher specific impulse, which is in the range of 10 to 50 km/s. This reduction in total fuel mass allows for bigger payloads mass, useful for long-term missions.

Although some EP thrusters use the same principle as conventional rockets, that is, heating a gas for a later expansion, the main focus of this project falls upon plasma thrusters, specially the Electron Cyclotron Resonace Thruster (ECRT), which will be discussed in detail in the following sections.

2.1 Plasma Physics

Plasma is considered to be the forth state of matter in the universe alongside solid, liquid and gas. Essentially, a plasma is a electrically charged gas, in which the electrons that form that gas have reached a sufficiently high energy, to be separated from the nuclei. What defines a separates plasmas from gases is that plasmas are fluids that are not in Local Thermodynamic Equilibrium (LET). The energy required to separate the electron from the nuclei is the ionization energy and it is a property of the considered gas. This electrically charged gas ,formed by electrons and ions, exhibits different characteristics that make plasma a different state. For instance, the fact that the charges can move independently, moving as an individual particles and not as a complete atom or molecule, makes plasma susceptible of interact with electromagnetic fields.

This energy required to ionized the gas can be provided by heat sources (heating the gas can create plasma; i.e stars), or by a strong electromagnetic field, capable to overcome the electromagnetic force that keeps the electrons orbiting.

Due to its nature, plasma needs a constant energy source, able to provide the required energy to sustain it. Otherwise, plasma will decay into a gas since the energy required to keep electrons and ions separated will dissipate due to collisions. This fact, along with the difficulty to create it in the first place it makes it really difficult its study and it has been in the last century when major discoveries of the plasma have been done, despite the fact that plasma is the most abundant state of matter in the universe.

2.2 Plasma Modelling Approaches

Physics behind plasma analysis usually involve complex equations that, except of oversimplified scenarios, numerical solutions are required to grasp the surface of its nature [9]. Different plasma models have evolved during the last century and, according to the type of analysis required, one model is preferred over another.

Kinetic Theory

Kinetic Theory is based on the idea that the plasma can be modelled as a distribution function $f(\mathbf{v}, \mathbf{x}, t)$ that resembles its behaviour in a 6D space as it specifies the average number of particles in the phase space volume $d\mathbf{r}d\mathbf{v}$. After some calculations involving this distribution function, Boltzmann equation arises:

$$\frac{\partial F_s}{\partial t} + \frac{\mathbf{p}_s}{m_s} \cdot \nabla f_s + q_s(\mathbf{E} + \mathbf{v} \times \mathbf{B}) \cdot \frac{\partial F_s}{\partial \mathbf{p}_s} = \left(\frac{\partial F_s}{\partial t}\right)_c \tag{2.1}$$

This equation shows how the distribution function changes inside a given control volume. It can be seen three contributions, the first one being the rate of change of the distribution function itself. Secondly, pressure forces driven by differences in pressure. Finally, the electromagnetic forces, represented by the Lorentz factor. The right hand side of the equation expressed the rate of change of the distribution function due to collisions. When this term is ignored, Vlasov equation arises as a simplification of the Boltzmann equation.

Subscript 's' describes a elementary particle population, in which particles that are part of that population share mass and charge. For an complete and close solution, Bolztmann equation is coupled with Maxwell equations.

This plasma model provides the highest amount of information possible since it tries to follow infinitesimal 6D space volumes over time. Due to this fact, numerical models that try to solve this distribution function requires great computational power and time. Only simplified scenarios can be studied with the help of this method.

PIC Models

Particle In Cell or PIC models divide the space domain in a mesh, so each particle is enclosed in a cell and in which parameters, such as the electric field, are computed at the nodes of the mesh, thus, a weighting method is needed to interpolate node's characteristics to particle position.

Usually PIC deals with what it is called macro-particles, a sort of combination of elementary particles, where the total mass or charge is due to the sum of each individual particle. Those macro-particles act as a cloud of particles that have similar movement. This allows PIC models to save in computational time at the cost of 'noise', statistical errors that do not exist in real plasma. The movement of these particles is influenced by external electromagnetic fields and the self-induced fields created by its own movement. Newton equation is then solved for each particle.

$$m_j \frac{d\mathbf{v}_j}{dt} = e[\mathbf{E}(\mathbf{r}_j) + \mathbf{v}_j \times \mathbf{B}(\mathbf{r}_j)] \tag{2.2}$$

Subscript 'j' represents a singular particle. Note that, electromagnetic fields should be updated at every time step as the position and velocity of the particles have changed. Numerical integrators such as the leapfrog model or the Boris scheme are used to solve Newton's equation.

Fluid Models

On the other hand, fluid models [10] simplify Kinetic Theory results by taking n^{th} velocity moments to the Bolztmann and Vlasov Equations, $\int v^n f(v,x,t) d^3\vec{v}$. For instance, by taking the zeroth, the first (with **v**) and the second moment (with $mv^2/2$), continuity equation, momentum balance and energy balance equations are obtained, respectively. Those equations resemble a typical analysis of Navier-Stoke's system of equations for fluids (hence the name) in which electromagnetic components have been added.

Some assumption that is usually made is that the distribution function of the particles adopts an isotropic Maxwellian function. This simplifies some calculations regarding heat flux and collisional terms. However, this assumption is only valid for highly collisional plasma. For low collisional regimes, solutions must be extracted from original equations.

Hybrid Models

In terms of complexity and results, Kinetic Theory offers more generic results than fluid models as those are based on a series of assumptions. Nevertheless, this comes with the price of more computational power required. Due to this reason, hybrid theories are being developed, which combines the two of them, in which some results are obtained by kinetic methods and some with fluid models. A compromise in terms of computational time and precise results must be done between the previously stated models.

Electron's mass is almost negligible, really close to zero, making them really difficult to track as little electromagnetic forces create large accelerations. Time steps required to fully track those electrons should be as low as possible for a detailed analysis. From a kinetic perspective, that will imply large computational times, however, as fluid models assume a macroscopic behaviour, no individual particles are followed.

Hybrid models takes advantage of this fact to create a combination, in which electron movement is derived by means of a fluid perspective while, on the other hand, ions, thousands of times more massive (thus, allowing for larger time intervals) are individually tracked with a kinetic or PIC model.

The development of these theories and models were a key success in the introduction of plasma in daily life. From plasma televisions to hydrogen production, plasma applications have changed the way the world works. As stated previously, the focus of this report is the analysis of the ECR, however it is important to locate the different modelling approaches amongst the different families of thrusters.

2.3 Plasma Thrusters

Space propulsion has evolved from solid propellant propulsion, used in the beginnings of the space era, to a more sophisticated propulsion type, EP. Due to the limitations in terms of limited thrust, this propulsion is not suitable for launching rockets, instead, it is employed in outer space, where drag is almost negligible, for station keeping maneuvers or maneuvers dealing with a change in a certain orbit.

Currently, more than a hundred satellites employed some kind of EP during its operational life. Cost-savings related to this propulsion make it a great focus of study nowadays, and this trend seems to be increasing since new models and engines are tested. As an example, NASA is currently working on two different ion thrusters, the NASA Evolutionary Xenon Thruster (NEXT) [11] and the Annular Engine, which in theory are capable of achieving great amount of thrust while increasing its lifetime. This will open new missions for EP satellites or spacecrafts never seen before.

Inside EP, a great variety of engines can be found, in which plasma thrusters play an important role. This type of thrusters create thrust by accelerating and expelling the particles the constitute the plasma, especially ions as the electron's mass are some orders of magnitude lower. This acceleration is produced by the electromagnetic effects that exist inside the engine's chamber.

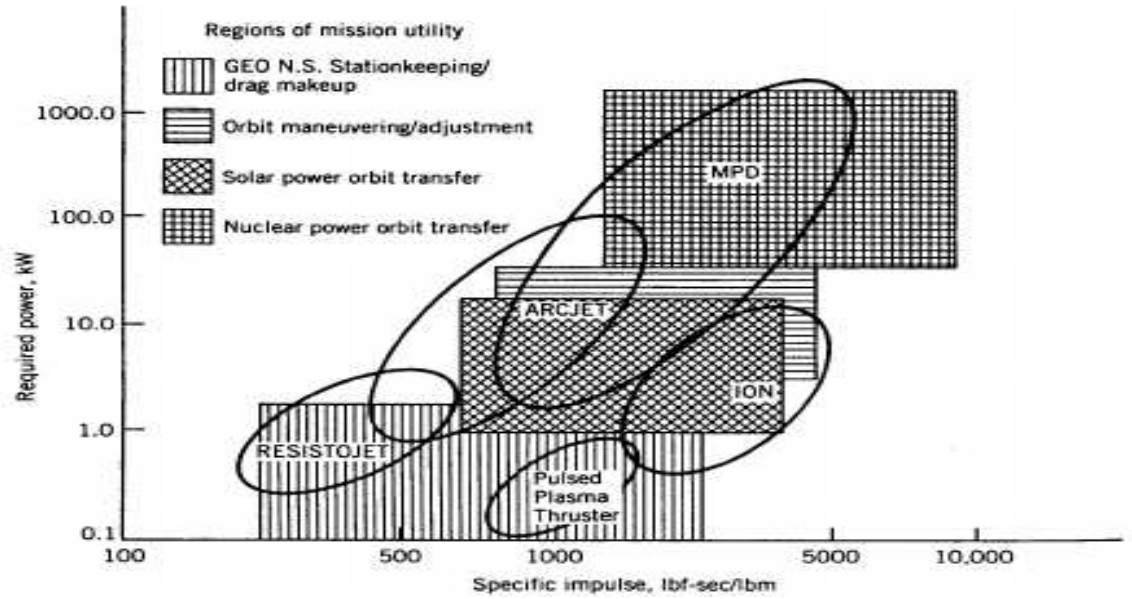

Figure 2.1: Distribution of different electric engines according to its power usage vs specific impulse [2]

Xenon is the most spread propellant over some other options in plasma thrust generation due to a series of reasons. First of all, it is a gas, that means that no energy is lost vaporizing the propellant for reaction purposes. Secondly, it is a noble gas,

hardly reacts with some other elements by definition. Xenon is heavy, with a mass of 131 unit of atomic mass. From basic rocket equations, the thrust is proportional to the mass flow rate of propellant exiting the chamber. Due to that reasoning, a heavier gas is preferred. Last but not least, ionization energy of xenon gas is relatively low, leading to minimum waste of energy creating the needed plasma. This characteristics make xenon the ideal gas for plasma thrust generation, although argon is typically used as well as it is less expensive than Xe due to its abundance in the atmosphere, but it is lighter.

Even though there exist electrothermal engines, whose principle of operation is based on heating a gas with electric power, increasing its pressure and then expanding it by means of a conventional nozzle, the ones regarding our attention are the family of thrusters which make use of electromagnetic fields to accelerate the plasma. This last group can be divided into electrostatic and electromagnetic engines. A brief introduction to the most important thrusters is given here.

Gridded Ion Thruster

Xenon propellant is injected in the engine chamber, which is then subjected to a bombardment of electrons, injected from a hollow cathode. Plasma is then created by the collisions between the highly energetic electrons and the propellant gas. Once that the plasma is created, ions are accelerated by a set of charged grids, that also serves as an electron confinement, continuously creating new ions. This ions are then ejected to the outer space, generating thrust.

This engine features great efficiency and high specific impulse compared to other types of thurster. However, it has some disadvantages as well. Main drawbacks can be found in the erosion of the grids due to the highly energy ion bombardment. Also, as only ions are expelled, some electrons need to be expelled (from another cathode, called the neutralizer) to the outer space to neutralize the increasingly positive charge density, that eventually will cease ion ejection. This cathodes erode rapidly and have limited lifetime.

Three different zones are appreciated here, the ionization region, the acceleration region due to the grids potential and a downstream neutralization region.

Hall Effect Thruster

Although these engines were envisioned more than fifty years ago, it was not until recently when substantial progresses were achieved, reaching a major step in 1994 when the first Hall Effect Thruster [12] was employed during a space mission.

Regarding the creation of plasma, these engines follow the same principle as the previous ones, that is, electron bombardment. However there exists a slight difference. The chamber of this engines has an anular shape, in which a radial magnetic field is created. This field, difficults the movement of the electrons towards the anode of the thuster as it creates an azimuthal movement, increasing the residence time of the electrons, which will colide a greater number of times with the propellant, leading to an increase of ionization efficiency. Finally, an axial electric field accelerates the ions for the creation of thrust. A neutralizer is needed due to the expulsion of a positive charge beam of ions.

Even though the operational principle of these kind of engines are based on a combination of magnetic and electric field, the way ions are accelerated is based on an axial electric field. This fact creates some controversy as how Hall Effect Thrusters are classified as some argue that due to how particles are accelerated they should be classified as electrostatic thrusters, while some experts exploit the fact that they use a combination of electromagnetic fields.

Helicon Plasma Thruster

One of the most recent plasma thruster to be born. Helicon Plasma thrusters [13] were firstly investigated during the 90's and current test are being carried by different investigation groups to test its feasibility in spacecraft missions. Its behaviour, similar to the ECR thruster is based on the absorption of electromagnetic wave energy by the electrons. This electromagnetic wave, produced by an antenna connected to a radio frequency power supply, capable of modulating wave properties accordingly to the plasma behaviour (frequency in the range of 1-27 MHz).

Once that the absorption of energy has been completed, electrons are accelerated by means of a magnetic nozzle, transforming perpendicular velocity into axial velocity, expelling ions due to the electric field created by the absence of negative charges. A neutral plume is then created, avoiding the use of a neutralizer.

Several prototypes are being currently tested in different facilities ranging from low power usage, a few watts to high power usage, around a few thousands of watts. We can find the Permanent Magnet Expanding Plasma (PEMP) or the Helicon Plasma Hydrazine COmbined Micro (HPHCOM), whose particularity is the used of permanent magnets. Some others are the Helicon Double Layer Thruster (HDLT), the mini Helicon Thruster eXperiment (mHTX) or the High Power Helicon Thruster (HPHT). Different measurements of thrust and efficiency for the different prototypes shows that more investigation is needed to determine what are the possibilities that Helicon Plasma Thruster offers.

Other engines

The previously mentioned thrusters, the Gridded Ion Thruster and the Hall Effect Thruster are the most spread electric engines nowadays. The have shown great efficiencies and specific impulsive that made those engines competitive in the current market. Helicon Plasma Thuster is a test engine greater results and has its view on the future. However, in the beginnings of EP, different engines were build.

In the early beginnings of the EP, the first engines were built based on the electrothermal principle. Resistojets and arcjets are examples of this kind of propulsion. Resistojets heat the propellant by means of a resistor, a filament subjected to a difference in potential that increases its temperature. The propellant is then expanded by means of a conventional mechanical nozzle. The main problem of this engine is is based on the filament itself. Due to material properties, there is a limit in the maximum amount of temperature in can be heated, bounding the maximum reachable temperature. Arcjets were designed to solve this problem. Arcjets heating principle is based on electric discharges from the center of the chamber. Thus, avoiding the use of the filament and increase the total maximum working temperature, directly related to the total thrust.

Lastly, it is important to mention the VAriable Secific Impulse Magnetoplasma Rocket (VASIMR), whose working principle is similar to the Helicon Plasma Thruster. However, it is based on the Ion Cyclotron Resonance, instead of the Electron Cyclotron Resonance. Due to the use of ions as the particles to heat, large magnetic fields are needed, as required by resonance. Finally, a magnetic nozzle accelerates the ions, which are expelled to create thrust.

Classification	
Electrothermal	Resistojet
	Arcjet
Electrostatic	Gridded Ion Thruster
	Hall Effect Thruster
Electromagnetic	Helicon Plasma Thruster
	VASIMIR
	ECR

Table 2.1: Classification of electric engines based on how propellant is accelerated

Electron Cyclotron Resonance Thruster

As its own name states, these thrusters are base on the concept of Electron Cyclotron Resonance Acceleration (ECRA), in which electrons are heated inside a chamber via electromagnetic waves coupling (microwaves, corresponding to frequencies of the order of GHz) and then accelerated using a magnetic nozzle thus, generating thrust due to the ambipolar electric field generated between the accelerated electrons and the ions.

The addition of the external fields has not only the advantage of accelerating the plasma for the creation of thrust, but also creates the condition for the microwaves to propagate through the plasma and deposit its energy to the electrons. At this particular position, where electrons are heated, the value of the magnetic field is known as the resonance magnetic field. At the same time, the presence of the magnetic field reduces the diffusion of the plasma species towards the walls of the thruster, limiting the energy losses to the wall. Lastly, magnetic field lines can be modified in orientation for some thrust vectoring, allowing the spacecraft to steer in the desired direction.

ECR thruster lies inside the group known as electrodeless engines. along with the Helicon Plasma Thruster (HPT). The innovation that these engines have brought to the industry, removing the cathode, allowed this type of engines to expand its lifetime as the associated problems of erosion are eliminated. As a whole, ECR engines are basic to manufacture (in terms of other electric engines), consisting only of a single chamber where ionization and heating occurs and a external divergent magnetic field, responsible for the acceleration.

ECR engines, due to its mechanism, presents several advantages over the traditional electric engines presented in the former section, in which we can find: simpler power units, throttleability, its thrust scales according to the power input and the ability of using several propellants such as xenon, argon or even oxygen (air-breathing operations are currently being studied). However it is important to highlight two of them:

- *The expelled plume consists not only of ions, but electrons too.* This neutrality of the plume allows for the elimination of the neutralizer, which, in the engines in which is used, limits the lifetime since it is prompt to suffer from erosion.

- *No need of some sort of grid to accelerate the ions.* Ions are accelerated by the ambipolar field caused by the expulsion of electrons. This reduces the total power supply needed for ion acceleration and increases lifetime as accelerating grids easily erodes.

Some losses mechanisms have to be solved to further complete the advantages that this engine provides. Inside those losses, one may find:

- Microwave power. Not all the input power transmitted by the power source is transformed in electrons kinetic energy. Although the conversion efficiency is high, some mechanisms losses appear at the resonance zone such as direct absorption of microwave energy or partial reflection of the wave
- Plume. Higher propulsive efficiency requires ions to be expelled axially in a uniform stream as fast as possible. However, plume divergence or non-uniformities of the plasma stream degrades the efficiency of the engine.
- Inonization. Ionization losses arise from the fact that, either, not all the propellant is completely ionized or after ionization, some ion-electron recombination occurs.
- Some others in which it can be found plasma interactions with the wall or energy losses due to plasma radiation.

Further research is needed for the completion of ECR. Nevertheless, the advantages and experiments carried out with this technology promise great results

3.1 Brief history of ECR

First experiments carried out that investigated this technology date back to the late 60's simultaneously by two different groups, one being the General Electric corporation funded by Lewis Research Center (LeRC) and another at the University of Tokyo. [14]

Early experiments carried out by these groups showed promising results. Different arrangements of ECR thruster with varying injection gases and several power levels were tested. During those experiments, it was measured a power deposition of 95% in the electron stream and a specific impulse of a few thousands. However, the controversy on how the experiments were mounted (where the gas injectors were placed, for instance) and the extraction of data lead to the repetition of the experiments, which yielded significantly lower results, although the experiments showed that the thermal energy was successfully transformed to kinetic energy due

to the external magnetic field. Some unknown losses while heating the particles were experienced.

In addition to that, at the time, power units responsible of producing and creating the electromagnetic power were massive and inefficient, while some other electric propulsion engines were successfully tested showing promising results. The study and further research of ECR thusters seemed to have found an end. However, the advancements done in the area of power units along with the improvement of numerical computational methods made possible the return of ECR investigation these two last decades with the creation of some ECR thruster prototypes such as ONERA [3], Sercel [15] and Miller, working at different power levels.

One of the first theoretical papers published that dealt with the problem of ECRA was Kosmahl's paper [16], released a few years after the first experiments were carried out. In this paper, Kosmahl, assuming a collisionless model, explained that the propulsive efficiency of the engine was highly dependant on the solenid's geometry, which defines the topology of the magnetic field. Large radial accelerations due to a great magnetic divergence, has a high influence on the total propulsive efficiency as an axial exit velocity is desired in terms of net thrust. Moreover, where the ionization and heating processes occur plays a major role here as he total acceleration that the plasma species experiences depends on the time that those particles are submerged in the magnetic field. An ionization region close to the backward plate of the engine allows for a greater acceleration than a further region.

Important participation in studying the acceleration mechanism was performed by Nagamoto at the University of Tokyo. Nagamoto, using only experimental methods, introduced several innovations when it comes to measuring relevant information. Its small non-intrusive measurement tools (hot Langmuir probes for instance) made for accurate measurements while keeping plasma flow and thruster capabilities unperturbed.

Nowadays, besides some groups studying the feasibility of ECR thrusters, the current trend of using ECR is focused on some atomic physics applications or plasma etching. Inside the first group, it can be highlighted fusion applications. Here, some plasma specie is trapped via magnetic confinement and continuously heated by ECR. Some differences are appreciable here. Fusion applications require higher magnetic fields (for confinement purposes) and thus, requiring power units capable of creating more energetic electromagnetic waves. Secondly, in terms of fusion applications thermal energy deposited via ECR must be transmitted to the ions instead of transforming it into axial velocity. This ion heating is the responsible of overcoming the strong nuclear interaction forces. In the end, the fusion application of ECR is being affected by the hig technical difficulties and the associated high energy sources needed. However, its study has helped the development of more efficient and powerful microwaves sources required for ECR thruster.

3.2 Configuration of an ECR thruster

As previously mentioned, the ECR thruster can be easily built in comparison with some other electrical devices of the same family. It can be decomposed in two different parts, an internal, where ionization and resonance occurs, and an external, where plasma is accelerated by an applied magnetic field.

Internal chamber

This internal chamber, whose dimensions and geometry vary according to the selected engine model, is fed of propellant (typically xenon or argon) by some input valves. This propellant is then ionized and heated by the corresponding microwave, which is produced by some electromagnetic device connected to a power unit. For instance, ONERA's model, circular in geometry, has included an antenna, located on its axis, which provides the required electromagnetic power.

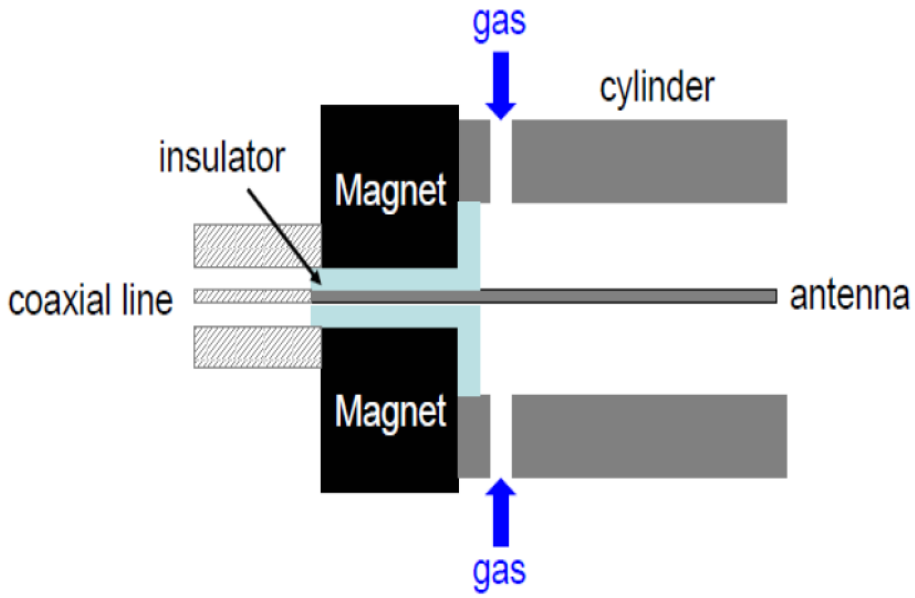

Figure 3.1: Schematic diagram of ONERA engine [3]

Once that the propellant has been successfully ionized, the electrons are heated via resonance, that is, the RHP wave resonates with the electrons, transferring its energy in a key process of the new elecrtodeless thrusters .

Let's start by a simplified case in which a charged particle moves under the presence of a constant uniform magnetic field. The Lorentz force is the expressed as:

$$\mathbf{F} = q(\mathbf{v} \times \mathbf{B}) \tag{3.1}$$

Notice that, due to the cross product, the force will always act perpendicular to both the magnetic field lines and the velocity, that is, the force will act on the perpendicular direction of motion, causing a rotation around the magnetic field lines. This circular motion, can be studied by the analysis of the centripetal force balance that acts on the particle as follows:

$$\frac{mv_\perp^2}{r_g} = ev_\perp B \rightarrow r_g = \frac{mv_\perp}{eB} \tag{3.2}$$

where r_g is the gyroradius or the Larmor radius. The frequency of rotation can be easily computed as follows:

$$f_{ce} = \frac{eB}{2\pi m} \tag{3.3}$$

This term is key because once that this frequency matches with the microwave frequency, resonance occurs. For that to happen, the magnetic field at resonance must satisfy the following expression:

$$f = f_{ce} \rightarrow B = \frac{2\pi f m_e}{e} \tag{3.4}$$

Once that the electron resonates with the wave, at the appropriate zone where resonance conditions meet, the electron sees a static electric field, its Larmor radius is increased and, thus, its perpendicular velocity increased, resulting in a net heating of the electron.

External zone: magnetic nozzle

The external zone of the ECR engine is composed of the external magnetic field. The magnetic field lines, created by two magnets or coils inside the chamber, diverges from the engine, creating a magnetic nozzle (MN). Slight variations into those coils or magnets make the magnetic lines to change direction allowing for thrust vectoring.

A magnetic nozzle follows the same principle as a magnetic mirror. Due to the magnetic gradient along the main axis, the particle interchanges its perpendicular velocity with axial kinetic energy, based on the conservation on the mechanical energy ε and adiabatic moment μ.

$$\varepsilon = \frac{1}{2}m_e v_\parallel^2 + \mu B \tag{3.5}$$

$$\mu = \frac{m_e v_\perp^2}{2B} \tag{3.6}$$

Similar to a mechanical nozzle, which transforms thermal energy from a hot gas into kinetic energy, magnetic nozzles transformed thermal energy of a plasma specie into axial kinetic energy useful for propulsive terms. Its ability to scale to high powers, due to its electrodeless nature, non limiting the useful life of this mechanism, has introduced MN into the electric propulsion market over the last few decades. Not only MN main advantage is the accelerating of the plasma but it also protects the engine preventing collisions with the walls of the thruster as the plasma species are forced to follow the magnetic field lines.

Electrons, considered to be magnetized due to the presence of the magnetic field are force to follow the magnetic field lines while being accelerated simultaneously. Due to the ambipolar effect caused by the absence of electrons, ions are forced to follow the electrons on their magnetic field line path. However, ions do not 'see' the magnetic field lines as electrons do since their mass is some orders of magnitude greater. Ions do not follow the magnetic lines, they follow the electrons.

It is well known that magnetic lines close onto themselves, so lines that come out of the engine must return to it. That means that electrons, and thus, ions, will travel all the way back to the engine, hitting the external walls and producing null thrust. Nevertheless, at some point, the acceleration of the ions is great enough so they can escape the path they go down, leaving behind the magnetic field and forcing electrons (in a similar way as ions are accelerated) to follow them. The plume is electrically neutral, so no neutralizer is needed.

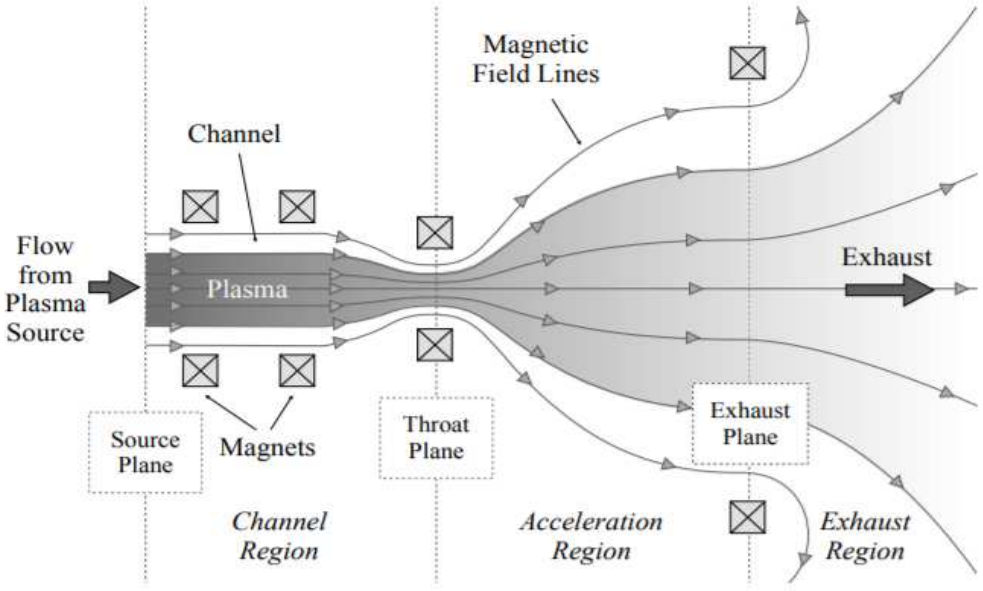

Figure 3.2: Typical magnetic nozzle configuration [4]

3.2.1 Magnetic nozzle analysis

Consider a situation in which a magnetic field with gradient exists in the absence of an electric field ($\mathbf{E} = 0$). This magnetic field satisfies the condition $\nabla\mathbf{B} \parallel \mathbf{B}$, stating that the gradient is parallel to a main axis of symmetry. Assuming also that no azimuthal magnetic field exists, the Lorentz force, expressed in cylindrical coordinates, is [17]:

$$\mathbf{F} = q \begin{vmatrix} \mathbf{r} & \boldsymbol{\theta} & \mathbf{z} \\ v_r & v_\theta & v_z \\ B_r & 0 & B_z \end{vmatrix} = \mathbf{r}(qv_\theta B_z) - \boldsymbol{\theta} q(v_r B_z - v_z B_r) - \mathbf{z}(qv_\theta B_r) \tag{3.7}$$

Taking a look to the last term of the equation, the radial magnetic field can be eliminated by applying the Maxwell equation $\nabla \cdot \mathbf{B} = 0$ in the radial form:

$$\nabla \cdot \mathbf{B} = 0 \rightarrow \frac{1}{r}\frac{\partial r B_r}{\partial r} + \frac{\partial B_z}{\partial z} = 0 \tag{3.8}$$

Assuming that the radial variable r is sufficiently small so that the gradient term $\frac{\partial B_z}{\partial z}$ can be considered to be constant, the radial magnetic field term can be integrated from the axial position to a distance r, resulting in the following expression

$$B_r = -\frac{r}{2}\frac{\partial B_z}{\partial z} \tag{3.9}$$

which, substituted into the axial force term yields

$$F_z = qv_\theta \frac{r}{2}\frac{\partial B_z}{\partial z} \tag{3.10}$$

This expression tells what is the force that a particle experiences on a given radial location, nevertheless, the information of the radial position of all the particle species may be hard to compute or to follow in a given system, so a way to eliminate the radial coordinate is needed. In order to do so, the radial term of the Lorentz force can be used. Notice that the radial force is not other that the centripetal force of the gyromotion in the following way:

$$F_r = qv_\theta B_z = -\frac{mv_\theta^2}{r} \rightarrow r = \frac{mv_\theta}{qB_z} \tag{3.11}$$

The negative sign is to point out that the radial force is directed inwards. Finally, this expression can be substituted into the axial force term as follows:

$$F_z = -\frac{1}{2}\frac{mv_\theta^2}{B_z}\frac{\partial B_z}{\partial z} \tag{3.12}$$

In a similar fashion, ignoring radial velocity terms, the expression for the azimuthal force is:

$$F_\theta = \frac{1}{2}\frac{mv_\theta v_z}{B_z}\frac{\partial B_z}{\partial z} \tag{3.13}$$

This expression of the axial force is the responsible of accelerating the charged particles in a magnetic nozzle and recalling that the magnetic field does not produce work on a particle since the applied Lorentz force acts in the perpendicular direction of motion, the net axial acceleration comes at the price of the perpendicular energy, keeping the total mechanical energy constant. It is interesting to see that the force is proportional to the magnetic gradient along the main axis and inversely proportional to the magnetic value. Greater values of the magnetic fields are not desired as the total acceleration will then be reduced.

Finally, the negative term in the former expression indicates that, in order to produce a net axial acceleration, the magnetic field must decrease along the axis direction. A decreasing magnetic field has two main advantages:

- Charged particles whose velocity is positive (along the main axis) are accelerated by the divergence of the magnetic field lines as seen.
- Particles travelling to the backplate of the magnetic nozzle (negative velocity) are, for the most part, reflected by the increasing magnetic field they experience. Only particle with high axial kinetic energies can overcome the magnetic field strength.

3.3 Brief introduction to the RHP

RPH wave stands for *Right Hand Polarized* wave and it is the one that provides the main heating mechanism in ECRT's, the so-called ECR heating (ECRH). As one of the major concenr of this type of electric propulsive engines, its study has become a major issue in the development of those thrusters. Its physics involved plasma-wave interaction, resulting in a specially difficult problem which has been researched since the late 60's. [18, 19]

A complete analysis comes from the study of Maxwell's equations coupled with kinetic theory to fully closed the problem. This equations encapsulates the core of plasma physics at it has been seen. Nevertheless the complexity of the full plasma model represented by this set of equations requires a extent knowledge of plasma behaviour and numerical analysis. These equations can be easily converted into a more convenient form by means of some simplifications and assumptions :

- Kinetic equations are linearized,
- Plasma is considered infinite and uniform,
- Plasma is treated as cold plasma.

With the introduction of the former simplifications,Fourier analysis allows the plasma contributions ρ_p and $\mathbf{j}_p$ to be expressed by a matrix tensor $\boldsymbol{\kappa}$, function only of the plasma frequency. Special careful must be taken with the cold plasma approximation, in which the thermal dispersion is considered negligible (that is, negelecting the contribution of the ions to the equations) as with this kind of approach, only essential information of the plasma behaviour, such as the resonance or cutoffs are conserved. For a more detailed analysis of the plasma-wave interaction (inhomogeneous plasma, non-linearities), Maxwell-Vlasov formulation is required.

By combining the Maxwell-Faraday and Maxwell-Ampere's equations, the magnetic field $\mathbf{B}$ can be eliminated, resulting in the following expression:

$$\nabla \times \left(\nabla \times \hat{\mathbf{E}}\right) = -\nabla^2 \hat{\mathbf{E}} + \nabla\left(\nabla \cdot \hat{\mathbf{E}}\right) = \frac{\omega^2}{c^2}\boldsymbol{\kappa} \cdot \hat{\mathbf{E}} + i\omega\mu_0 \hat{\mathbf{j}}_a \tag{3.14}$$

where $\mathbf{E}$ has been expanded into the wave number domain:

$\mathbf{E} = \Re[\tilde{\mathbf{E}} exp(i\mathbf{k}\cdot\mathbf{r} - i\omega t)]$

resulting in:

$$\left[\begin{pmatrix} -k_y^2 - k_z^2 & k_x k_y & k_x k_z \\ k_x k_y & -k_x^2 - k_z^2 & k_y k_z \\ k_x k_z & k_y k_z & -k_x^2 - k_y^2 \end{pmatrix} + \frac{\omega^2}{c^2}\begin{pmatrix} \kappa_{xx} & \kappa_{xy} & \kappa_{xz} \\ \kappa_{yx} & \kappa_{yy} & \kappa_{yz} \\ \kappa_{zx} & \kappa_{zy} & \kappa_{zz} \end{pmatrix}\right] \cdot \begin{bmatrix} \tilde{E}_x \\ \tilde{E}_y \\ \tilde{E}_z \end{bmatrix} = -i\omega\mu_0 \begin{bmatrix} \tilde{j_{ax}} \\ \tilde{j_{ay}} \\ \tilde{j_{az}} \end{bmatrix} \tag{3.15}$$

in which a orthogonal complex basis exists as:

$$\mathbf{e}_+ = \begin{bmatrix} 1 \\ -1 \\ 0 \end{bmatrix}, \mathbf{e}_- = \begin{bmatrix} 1 \\ i \\ 0 \end{bmatrix}, \mathbf{e}_z = \begin{bmatrix} 0 \\ 0 \\ 1 \end{bmatrix} \tag{3.16}$$

The matrix tensor $\boldsymbol{\kappa}$, expressed in this basis is diagonal:

$$\boldsymbol{\kappa} = \begin{bmatrix} L & 0 & 0 \\ 0 & R & 0 \\ 0 & 0 & P \end{bmatrix} \tag{3.17}$$

where L stands for "left", R for "right" and P for "plasma", representing both the left and right hand side terms of the electromagnetic wave and the plasma oscillations

$$L = 1 - \sum_s \frac{\omega_{ps}^2}{\omega(\omega + i\nu_e \mp \omega_{cs})}, R = 1 - \sum_s \frac{\omega_{ps}^2}{\omega(\omega + i\nu_e \pm \omega_{cs})}, P = 1 - \sum_s \frac{\omega_{ps}^2}{\omega(\omega + i\nu_e)} \tag{3.18}$$

where ν_e is the effective collisionality term of the electron especies. Notice the dependant on the expressions of plasma characteristic parameters (of specie s) such as the plasma frequency ω_{ps} or the gyrofrequency ω_{cs} expressed as:

$$\omega_{ps}^2 = \frac{e^2 n_0}{\epsilon_0 m_e} \; and \; \omega_{cs} = \frac{eB_0}{m_e} \tag{3.19}$$

The evolution of the RHP can be studied by the simplified one-dimensional wave equation. It is important to remark that ion contribution to that equation can be neglected. It can be seen that the mass of the specie affects the previous parameters of that plasma specie. Having a much greater mass results in negligible frequencies compared to those of the electrons.

$$\frac{d^2 E_-}{dz^2} + \frac{\omega^2}{c^2}\left(1 - \frac{\omega_{pe}^2(z)}{\omega[\omega - \omega_{ce}(z) + i\nu_e(z)]}\right) E_- = 0 \tag{3.20}$$

Up from here, some simplifications can be made to analytically solve this equation such us the magnetic field profile (which will determine the gyrofrequency of the electrons). Otherwise, numerical solvers are needed, updating at each time step the plasma parameters of the equation.

From the analysis of the RHP wave, it has been seen that the presence of a external magnetic field affects its propagation and resonance. Two main cases can be explored and analyzed, though only a brief explanation is given here: (i) wave propagating through a increasing magnetic field and (ii) wave propagating through a decreasing magnetic field.

For case i, it has been seen that an increasing magnetic field seen by the microwave provokes a reflection of the wave at the resonance zone while some is transmitted. For case ii, no reflection of the wave is experienced. These reflected and transmitted energies are dependant on the plasma and magnetic field profiles. For the case i, the incoming wave encounters the reflected one, whose contributions are added accordingly. In any case, the transmitted energy seems to be exactly the same independently of the magnetic gradient. Nevertheless, some energy is absorbed by the resonance region and deposited to the electrons. Case ii configurations are used in real ECR thrusters due to the greater energy deposit at the resonance.

To conclude, a simplified analysis of the RHP wave has been presented here. It has been demonstrated that the RHP wave is influenced by plasma parameters, as well as the external magnetic field. Adjusting this variables in a ECR thruster become key in the development of a efficient engine. Thus, in order to fully solve the equation, a complete description of the plasma is necessary as not only RHP is a function of space as 3.20 shows but a function of time as collisions, and plasma frequencies evolves according to the plasma properties.

PIC and mover modelling

Previously, a brief introduction on the mechanism of PIC codes was introduced. It was stated that particles were weight in some kind of mesh that divides the domain in a fixed number of grids. This section is devoted for a further explanation of this type of codes, how they work and why are they useful.

Effectiveness and usefulness of PIC codes have been greatly proved since it early beginnings in the 50's. Numerical kinetic plasma simulations have been investigated by PIC models in which we include, laser-plasma accelerations, fusion investigation in tokamaks, phenomena occurring at the ionosphere... Its versatility and functionality make it useful for a great variety of kinetic plasma simulations.

Its power comes from the fact that the bulk number of particles to follow is decreased drastically compared with standard kinetic models as PIC codes deal with macroparticles, which can be physically understood as a cloud of real particles with similar movement.

Although some of the advantages that PIC codes provide are extremely useful (nonlinear effects can be studied, not boundary conditions along $\mathbf{v}$...), their applications are mostly constrained to collisionless plasma and some statistical errors are intrinsic of this type of codes, in which we can find for instance some noise introduced by the weighting of the particles, or the limitations introduced by a grid, which turns out to be a severe constraint in the study of relativistic plasmas.

4.1 Summary of a self-consistent PIC code

PIC codes are based on a loop. When the particles' position and velocities are known, it is possible to calculate the electromagnetic fields that they generate and that are the responsible for their movement. Once that that is known, the mover plays its role updating particles' information. With this new information, the fields are then updated for another particle mover interaction. Following Figure schematizes this loop.

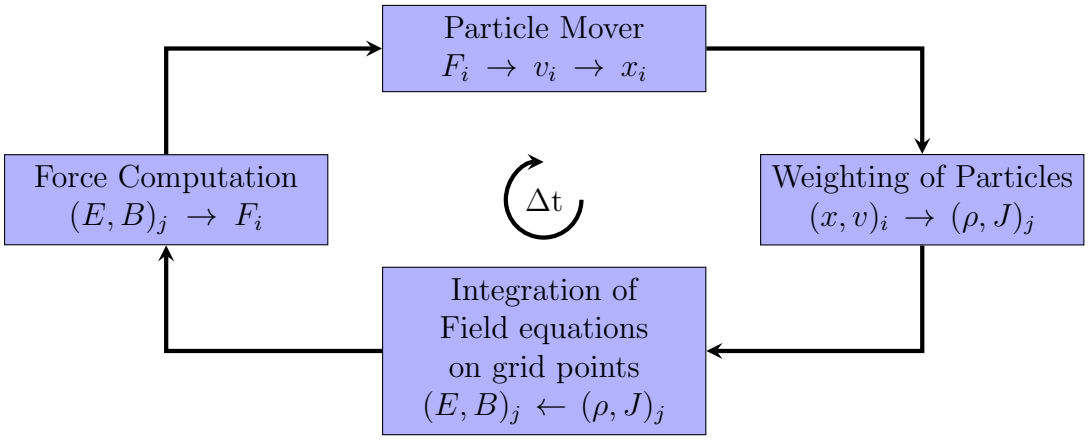

Figure 4.1: PIC logical loop. Subscript 'j' represents nodal positions and subscript 'i' represents particle position

This complete loop results in a complete and self-consistent solution of the movement of the particles as it takes into account both the electromagnetic fields that are created due to the own plasma movement and the external applied fields.

4.2 Particle mover

A particle mover is based on the fact that, given the different forces that act on a particle and an initial condition for the position and the velocity, the trajectory of that particle for a determined time is computed. This whole process is based on Newton's equation, which states that the rate of change of the velocity is proportional to the applied force and inversely proportional to the particle's mass.

Solving Newton's equation is not a trivial task, as it involves a vector differential equation that combines the contribution of the electrostatic force together with the magnetostatic Lorentz force. Regarding computational time, the particle mover is the section of the code which requires more power and time to solve for the particle position and velocity. In that sense, the use of an effective, quick and accurate method is key for the performance of the particle in cell code. In that sense, two different algorithms have demonstrated its effectiveness, the leapfrog scheme and the Buneman-Boris method.

4.2.1 Leapfrog scheme

Consisting in some Euler numerical analysis (*finite difference substitution*), Newton equation is divided into:

$$\frac{d\mathbf{x}}{dt} = \mathbf{v} \tag{4.1}$$

$$\frac{d\mathbf{v}}{dt} = \frac{\mathbf{F}}{m} \tag{4.2}$$

After substitution, the resultant finite differences are

$$\frac{\mathbf{x}^{t+\Delta T} - \mathbf{x}^{t}}{\Delta T} = \mathbf{v}^{t+\Delta T/2} \tag{4.3}$$

$$\frac{\mathbf{v}^{t+\Delta T/2} - \mathbf{v}^{t-\Delta T/2}}{\Delta T} = \frac{\mathbf{F}^{t}}{m} \tag{4.4}$$

Notice the time fractions superscript on the velocity components arises from the fact of using finite differences. In order to start with this scheme, the user should translate the velocity component from t=0 to t=-$\Delta T/2$ by applying half Euler difference using the fields at t=0; then the scheme can run.

Although simplistic on its form, leapfrog scheme provides really good and surprisingly accurate results. As a numerical model, the error goes to zero as $\Delta T \to 0$.

4.2.2 Buneman-Boris method

Often simplified as Boris method, this method is an elegant alternative to leapfrog schemes which, with the addition of magnetic fields, becomes hard and not easy to implement due to the cross product term. Let's recall the equation to solve:

$$\frac{\mathbf{v}^{t+\Delta T/2} - \mathbf{v}^{t-\Delta T/2}}{\Delta T} = \frac{q}{m}\left[\mathbf{E} + \frac{\mathbf{v}^{t+\Delta T/2} + \mathbf{v}^{t-\Delta T/2}}{2} \times \mathbf{B}\right] \tag{4.5}$$

in which implicit forward difference of Newton's equation have been applied. Notice that the introduction of the cross product term increases the difficulty of finding an analytic solution. A clever way to eliminate the electric field of the equation an thus, transforming the movement into a rotation, is to define the following intermediate velocities:

$$\mathbf{v}^{t-\Delta T/2} = \mathbf{v}^{-} - \alpha\mathbf{E} \tag{4.6}$$

$$\mathbf{v}^{t+\Delta T/2} = \mathbf{v}^{+} + \alpha\mathbf{E} \tag{4.7}$$

where α is defined as:

$$\alpha = \frac{q\Delta T}{2m}$$

plugging those definitions in Equation 4.5, the resultant expression is:

$$\frac{\mathbf{v}^{+} - \mathbf{v}^{-}}{\Delta T} = \frac{q}{2m}(\mathbf{v}^{+} + \mathbf{v}^{-}) \times \mathbf{B} \tag{4.8}$$

The steps to solve Boris method are: add half acceleration due to the electric field indicated by Equation 4.6, perform the full rotation indicated by 4.8 and adding the remainder half acceleration as 4.7 dictates. Step two of this method can be further split by paying attention to the geometry of the rotation. The angle of rotation is given by $\tan(\theta/2) = -qB\Delta T/2m$ which, in vector form is $\mathbf{t} = q\mathbf{B}\Delta T/2m$. With this information is easy to obtain a close solution of $\mathbf{v}^{+}$

$$\mathbf{v}^{+} = \mathbf{v}^{-} + (\mathbf{v}^{-} + \mathbf{v}^{-} \times \mathbf{t}) \times \mathbf{s} \tag{4.9}$$

where $\mathbf{s}$ is just the rotation vector $\mathbf{t}$ scaled to satisfy a constant magnitude rotation given by the following expression:

$$\mathbf{s} = \frac{2\mathbf{t}}{1 + t^2} \tag{4.10}$$

Boris' method offers an easy and close analytical form of solving Newton's equation that, although requiring more computational time than the leapfrog scheme, offers great accuracy at the expenses of a few more steps. This method was implemented and tested for different cases involving different configurations of electromagnatic fields, however, due to the nature of the RHP, which acts in the perpendicular direction of the movement, a different mover was finally implemented for the simulations

4.2.3 Particle Mover with the effect of the RHP

The previously mentioned movers are employed for movements on particles confined in a 1D region due to its robust behaviour and efficiency. However, due to the nature of the RHP wave, extra details are necessary to fully understand its behaviour and interaction with the plasma. In that sense, it is necessary to create a polar coordinate system in which the x-axis corresponds to the longitudinal axis and the y and z-axis correspond to the perpendicular axis, following the right hand side rule. In this coordinate system, it is possible to define two velocities, one parallel to the longitudinal axis and another perpendicular to it, such that:

$$v_{\parallel} = v_x \tag{4.11}$$

$$v_{\perp} = \sqrt{v_y^2 + v_x^2} \tag{4.12}$$

Now, the forces that act on the particle must be traced in order to follow the particle's evolution. These forces have two different sources, one being the electric field and the other the magnetic field. The final differential equations to be solved are:

$$\frac{dv_{\parallel}}{dt} = \frac{eE}{m} - \frac{v_{\perp}^2}{2B_z}\frac{\partial B_z}{\partial z} - \nu_{\parallel} v_{\parallel} \tag{4.13}$$

$$\frac{dx}{dt} = v_{\parallel} \tag{4.14}$$

$$\frac{dv_{\perp}}{dt} = \frac{eE_R}{m}\cos(\alpha - \beta) + \frac{v_{\parallel} v_{\perp}}{2B_z}\frac{\partial B_z}{\partial z} - \nu_{\perp} v_{\perp} \tag{4.15}$$

$$\frac{d\beta}{dt} = \frac{-eB_z}{m} + \frac{eE_R \sin(\alpha - \beta)}{m v_{\perp}} \tag{4.16}$$

This set of differential equations will define the movement of a particle inside a domain in which a RHP wave is present. A division between parallel and perpendicular axis is made to explain where each term of the equations comes from.

Parallel axis

Let's start by stating the forces that act on the parallel axis due to the presence of an electromagnetic field. The simplest one consists of an axial electric field that, according to the corresponding Lorentz force is:

$$\mathbf{F} = e\mathbf{E} \tag{4.17}$$

stating that positive electric fields will accelerate ions in the positive direction and accelerate electrons in the negative direction. Secondly, the force due to the axial magnetic nozzle. Recalling the expression of Equation 3.12, an additional term accounting for the divergence of the magnetic field is included. Finally, according to the definition of velocity, the particle position along the parallel axis is updated as 4.14 states.

Perpendicular Axis

For the case of the perpendicular axis, the evolution of the perpendicular velocity is more difficult to express, as the perpendicular electric field acting is the RHP wave, which rotates with an angular velocity determined by its frequency. In this case, let's call α the angle that the RHP makes with the y axis and, in a similar fashion, β is the angle formed by the perpendicular velocity as the following Figure shows:

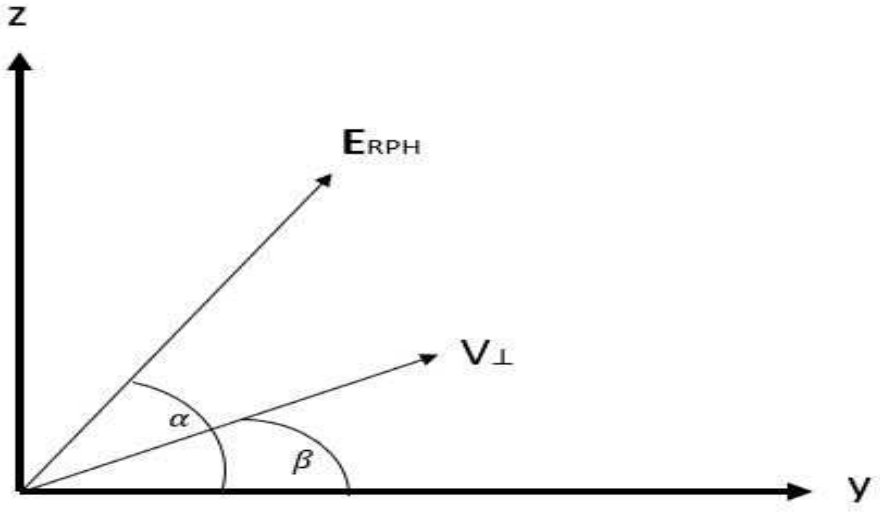

Figure 4.2: Coordinate system for perpendicular direction

Firstly, resonance occurs when these two angles are the same and its evolution follows the same rate. In that case, the electron will see a stationary electric field and will be accelerated in the perpendicular direction. Otherwise, the electric filed will act on the perpendicular velocity depending on the difference between the two angles. Secondly, the next force acting on this direction is given by Equation 3.13, due to the presence of the magnetic field.

The time derivative of the β angle has two components, one being the gyromotion due to the presence of the magnetic field as expression 3.19 dictates. The second term is dependent on the presence of the RHP wave. The evolution results in:

The evolution of the angle α is dictated by the frequency of the RHP wave. Recall that this wave can be seen as a perpendicular electric field which is rotating at a given frequency.

$$\frac{d\alpha}{dt} = \omega_{RHP} \tag{4.18}$$

An additional term can be added to the velocity equations to account for the collisions of the particles. This term, proportional to the velocity of the particle, expressed that the greater the velocity, the greater the energy loss due to collisions with the background plasma. The proportionality constant, named collisional frequency, with units of s^{-1} rules the loss of momentum. At the end, the system of differential equations must be solved for a close solution of the problem.

In order to do so, a custom *Matlab* code has been implemented by the use of in-built functions. These kind of functions integrates first order differential equations by applying a Runge-Kutta method on a given t_{span} of the form of:

$$\frac{d\mathbf{x}}{dt} = \mathbf{f}(t, \mathbf{x}), \qquad \mathbf{x}(t_0) = \mathbf{x}_0 \tag{4.19}$$

These *Matlab* in-built functions solve the problem using a variable time step numerical scheme integrator, in which the stated function solves the differential equations in a way such that the total t_{span} is divided into smaller time steps, whose size depends on the required tolerances. That is, the step size varies to meet tolerance requirements.

4.3 Mechanism of a 1D PIC code

Charged particle's trajectories are influenced by electromagnetic fields. Those fields exert some forces on the particle according to the electrostatic force (for the electric field) and the Lorentz force (for the magnetic field case). For this last case, the force that a magnetic field exert onto a particle depends on the velocity components of that particle trajectory, resulting in a indispensable requirement the computation of that velocity components. On top of that, the computation of those fields are dependent on the velocity components as well, since the current density is defined based on the velocity.

For one dimension (direction of propagation: x-axis)

$$\frac{\partial}{\partial y} = \frac{\partial}{\partial z} = 0$$

This condition implies that fields and current are only dependent on the x coordinate, leaving the rest of coordinates free-dependent.

However, different studies may require different PIC codes. For instance, the DRACO code developed for the modeling of electric propulsion in plasma plume interactions is a fully 3D code in which the simplification made by the 1D code is disregarded. At the end, it is a matter of selecting the most suitable code for a given project.

PIC codes, regardless of their type always start by defining a domain of study. Is in that domain where the space is discretized using a mesh. For this particular case, as the domain is constraint to be in one dimension, it is just a straight line, divided in uniform segments of length ΔX. Typically, for plasma analysis with electromagnetic interaction, this ΔX segments are of the order of the Debye length of the plasma, which is defined as:

$$\Delta X \sim \lambda_d = \sqrt{\frac{\epsilon_o k_B T}{n_e q_e^2}} \tag{4.20}$$

where ϵ_o is the permittivity of free space, k_B is the Boltzmann constant, T is the temperature, n_e is the electron density and q_e is the elementary charge.

As the method of solving Maxwell and Newton equations are based on numerical center finite difference, a time step ΔT is also necessary. However, this comes with the constraint of satisfying the so-called Courant condition. This condition forces the time step to be below some numerical value for convergence purposes. Courant condition is as follows[20]

$$C = \frac{u\Delta T}{\Delta X} \leq C_{max} \tag{4.21}$$

where u is the propagation velocity of the scheme, which turns out to be c for plasma interactions. C_{max} usually takes the value of 1, however matrix solvers are less prompt to instabilities, so larger values are tolerated.

Once that the domain has been established, loading of the charge particles comes next. This may be done arbitrarily, setting the initial position and velocity as the user requests. Maybe the initial particles follow Maxwellian distribution function, or the user may state that at some intervals new particles are injected at a particular rate to the domain.

4.3.1 Weighting of particles

Particles in PIC codes interact with the mesh through densities and currents and the mesh interact with particles through electromagnetic fields. In that way, the mesh is used to compute the value of the electromagnetic fields at each node, based on the quantities expressed by the plasma. How this computation is realized is based on the weighting method, a way to express densities onto the grid nodes of a given population at a given instant in time. That is what differentiates PIC codes from other codes, its capability of expressing plasma quantities onto a grid via weighting.

Different ways of weightings may be employed, ranging from its simple form to arbitrarily difficult ways:

Zero-order weighting

Also called *nearest-grid-point* or NGP, this system works by accounting for the number of particles lying from a distance $\pm\Delta X/2$ about the j^{th} grid point, so for instance, the particle density is simply computed as:

$$n_j = \frac{N(j)}{\Delta X}$$

Although easy to implement and fast regarding computational time, NGP weighting system will create rectangular shapes at each grid point, leading to the origin of 'jumps' as a particle passes through a cell boundary. This effect produces some noisy effect that may lead to non-physical effects, obviously intolerable to some plasma interactions.

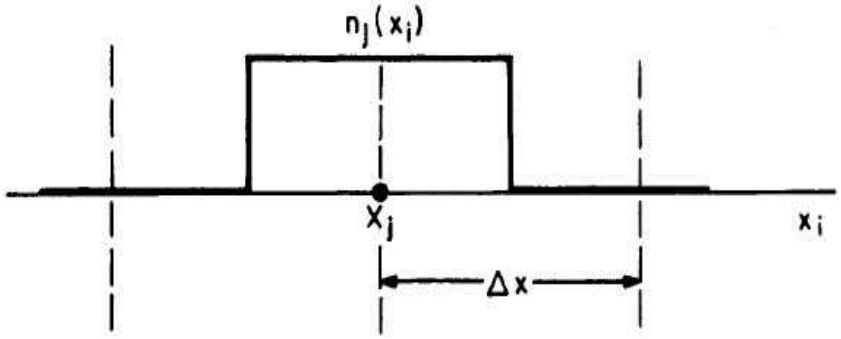

Figure 4.3: Zero-order scheme [5]

First-order weighting

Instead of accessing one grid point per particle, this system will have to access to two different grid points per particle as the first-order weighting has a triangular shape and the particle properties are interpolated to the closest grid points as follows:

$$S(x_i - x_j) = \begin{cases} 1 - \frac{|x_i - x_j|}{\Delta X} & if \qquad x_i - x_j \leq \Delta X \\ \\ 0 & elsewhere \end{cases} \tag{4.22}$$

This weighting method states that if the particle position is exactly at the grid point, all of its information will be then translated to that grid point. The farther the particle is from that grid point, the less contribution to that node, while the approaching node will be more important. If the particle's position is greater than ΔX, then, the grid point is unable to see the particle's properties. This transition from node to node resembles the movement of a cloud as the particle travels freely. Due to that, first-order weighting is also called *cloud-in-cell* or CIC.

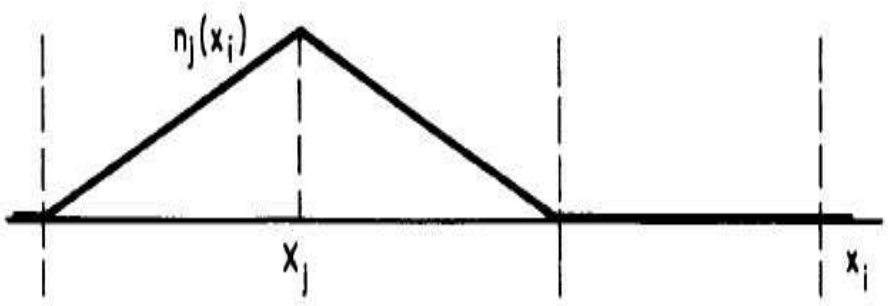

Figure 4.4: First-order scheme [5]

With the addition of this type of weighting, the transition from grid point to grid point as a particle moves is much smother, reducing the amount of noise that the weighting system generates. It is true that this system will require more computational time to weight particle's properties, as it has to access to two grid points, however, the reduction in noise level allows this system the capability of introducing less grid points or less particles.

Higher order weightings

Quadratic, cubic and higher order splines are located around a given grid points, reducing the noise by attenuating the roughness of the shape. The cost of this higher order weightings comes at the price of more computational time and at some point, the increase in accuracy due to increase the order is negligibly small compared to the increased in computational power. For this simulation, CIC weighting system is used, given enough information about the plasma analysis.

4.3.2 Fields computation

Particles inside PIC codes moves according to Newton's equation, as previously stated. According to that equation, the rate of change of the velocity is proportional to the electromagnetic fields, either external fields or self-induced fields due to the movement of the particle. A combination of both is also possible.

So in order to solve Newton's equation, it is mandatory to compute the fields that act on each particle by solving Maxwell's equation, which are secondly presented here as a reminder.

$$\nabla \cdot \mathbf{B} = 0 \tag{4.23}$$

$$\nabla \cdot \mathbf{E} = \frac{\rho_c}{\epsilon_0} \tag{4.24}$$

$$\nabla \times \mathbf{E} = -\frac{\partial \mathbf{B}}{\partial t} \tag{4.25}$$

$$\nabla \times \mathbf{B} = \mu_0 \mathbf{j} + \frac{1}{c^2}\frac{\partial \mathbf{E}}{\partial t} \tag{4.26}$$

Equation 4.23 (**Gauss Law for Magnetism**) states that the divergence of a magnetic field is null, that is, either the field lines closes to themselves or they are infinite. By this definition, no sinks or sources of magnetic field lines exist.

Equation 4.24 (**Gauss Law for Electricity**), unlike the previous one, states that sinks and sources of electric field do exist, being positive charges sources and negative charges sinks.

Equation 4.25 (**Maxwell-Faraday's Law**) talks about how a time-variance change in the magnetic field provokes a rotation in the electric field.

Finally, Equation 4.26 (**Maxwell-Ampere's Law**) expresses a similar conclusion as the Maxwell-Faraday's Law, saying that the magnetic field is altered by the presence of currents, either currents created by the movement of charges or by the time-variation of the electric field.

Assuming a steady evolution of the magnetic field, that is considering an irrotational electric field as Equation 4.25 is set to zero, it is possible to define a scalar function named the electric potential function as follows:

$$\mathbf{E} = -\nabla \varphi \tag{4.27}$$

The derivation of what it is called Poisson's equation arises by the combination of this expression with the Gauss Law equation for electricity:

$$\nabla \cdot \mathbf{E} = \nabla \cdot (-\nabla\varphi) = -\nabla^2\varphi = \frac{\rho_c}{\epsilon_0} \tag{4.28}$$

By applying the Poisson's equation of electricity, it is possible to numerically obtain the electric potential of a given charged population of particles. With that potential, the electric field can be easily obtained. By considering that the implemented code is only available in one dimension, Poisson's equation is reduced to a second partial derivative with respect to the x position, which can be numerically solved by applying second finite differences as follows:

$$\frac{\partial^2\varphi}{\partial x^2} \approx \frac{\varphi_{j+1} - 2\varphi_j + \varphi_{j+1}}{\Delta X^2} = -\frac{\rho_j}{\epsilon_0} \tag{4.29}$$

where 'j' represents grid position. For a given domain, which has been divided into a finite number of cells for which the charge density is known at each grid point, it is possible, with the appropriate boundary conditions, to obtain the potential field of the distribution. A way to solve Poisson's equation is by the use of matrices and solving a system of equations of the form:

$$A\mathbf{x} = B \tag{4.30}$$

where A is the coefficient matrix, $\mathbf{x}$ is the vector of unknowns and B is the result vector. Those terms are expressed as:

$$A = \begin{bmatrix} 2 & -1 & 0 & 0 & \cdots & 0 \\ -1 & 2 & -1 & 0 & \cdots & 0 \\ 0 & -1 & 2 & -1 & \cdots & 0 \\ \vdots & & & & \ddots & \\ 0 & \cdots & & 0 & -1 & 2 \end{bmatrix} ; \mathbf{x} = \begin{bmatrix} \varphi_1 \\ \varphi_2 \\ \varphi_3 \\ \vdots \\ \varphi_n \end{bmatrix} ; B = \frac{\Delta X^2}{\epsilon_0} \begin{bmatrix} \rho_1 - \frac{c_1\epsilon_0}{\Delta X^2} \\ \rho_2 \\ \rho_3 \\ \vdots \\ \rho_n - \frac{c_2\epsilon_0}{\Delta X^2} \end{bmatrix} \tag{4.31}$$

In this expression, c_1 and c_2 are the boundary conditions at the limits of the domain. They are selected according to the properties of the problem. This definition of boundary condition is named Dirichlet conditions, in which the solution of the electric potential is set. Dirichlet conditions are chosen since the potential can be easily set at the boundaries of a real project. Of course, different boundary conditions can be chosen , however those are out of the scope of this project. Once that the electric potential is known, the extraction of the electric field is computed as follows:

$$\frac{E_{j+1} - E_{j-1}}{2\Delta X} = \varphi_j \tag{4.32}$$

where a centered finite difference is employed. For the beginning and ending of the domain, forward and backward differences are used respectively. For this simulation, it has been assumed that the moving particles do not create a magnetic field as the Maxwell-Ampere's law states for simplicity. However, for a complete solution of the problem, the whole set of Maxwell's equations ought to be solved. Applying the 1D condition, the system of equations turns out as:

$$\frac{\partial B_x}{\partial x} = 0 \rightarrow B_x = cte \tag{4.33}$$

$$\frac{\partial E_x}{\partial x} = \frac{\rho}{\epsilon_0} \tag{4.34}$$

$$\frac{\partial E_z}{\partial x} = \frac{\partial B_y}{\partial t} \;/\!/\; \frac{\partial E_y}{\partial x} = -\frac{\partial B_z}{\partial t} \tag{4.35}$$

$$-\frac{\partial B_z}{\partial x} = \mu_0 j_y + \frac{1}{c^2}\frac{\partial E_y}{\partial t} \;/\!/\; -\frac{\partial B_y}{\partial x} = \mu_0 j_z + \frac{1}{c^2}\frac{\partial E_z}{\partial t} \tag{4.36}$$

Notice how the difficulty increases if time evolution is considered as not only finite differences in space should be computed but in time as well. That means that not only the initial conditions must be defined, but the previous step as well. This can be done by calculating what were those previous conditions based on the next step. However that is out of the scope of this project.

Taking a look to the Maxwell's equations, it is clearly seen that the first step to compute the electromagnetic fields is the extraction of charge densities and current densities.

Extraction of charge and current densities (ρ and j)

Let's start by defining what it is charge and current densities before computing them. Firstly, charge density is defined as the amount of electric charge per unit of length, surface or volume, depending on the dimensions of the problem. For this case, it is defined per unit length, measured in $C \cdot m^{-1}$. As for current density, it is defined as the flow of electric charge per unit of area in a three dimensional volume $[A \cdot m^{-2}]$. Its computation its simply done by multiplying the charge density by the velocity of the particle (from that, its vector nature).

Making use of the CIC weighting system, the total charge density per grid point is computed as:

$$\rho_j = \sum_{i}^{Np} q_j S(x_i - x_j) \tag{4.37}$$

where, again, subscript 'j' indicates grid parameter and 'i' represents particle properties. Np represents the total number of particles in the domain.

Similarly, current density is computed as:

$$\mathbf{j}_j = \sum_i^{Np} q_j \mathbf{v}_i S(x_i - x_j) \tag{4.38}$$

Notice that with this definition of densities, the equation of continuity is automatically satisfied. Recalling this expression, let's remark that this continuity equation arises from the fact that the charge is conserved. [21, 22]

$$\nabla \cdot \mathbf{j} = \sum_i^{Np} q_j \mathbf{v}_i \nabla \cdot S(x_i - x_j) = -\frac{\partial \rho}{\partial t} \tag{4.39}$$

This continuity equation states that the variation of charge inside a volume is due to movement of the charged particles inside of it, leaving or entering the control volume.

Results

In order to validate the performance of the code, some test are run to check the performance of the code. The run of this test codes, consisting in a magnetic bottle analysis that facilitates the validity of the whole operation since checking the correct operation of code groups will allow to fix the errors that may arise. Finally, simulation results are shown using the solution that arises from Equation 3.20 for a representative case, an underdense plasmas scenario.

5.1 Validation simulations

5.1.1 Magnetic Bottle

One of the test to be run is the creation of a magnetic bottle. Equations of motion described on the previous section will be proven to validate a well know test, with a defined analytical solution.

The use of magnetic fields to trap charged particles was first proposed in the mid 50s and has evolved and refined since by increasing its performance, reducing dumping effects and noticeably decreasing power input. Its foundations are based on the Lorentz force, the force produced by a magnetic field onto a charged particle. This magnetic field can be produced by two coils separated by a distance L by which a electric current circulates.

$$\mathbf{F} = q \cdot (\mathbf{v} \times \mathbf{B}) \tag{5.1}$$

Due to the geometry of the magnetic field, this Lorentz force is always pointing to the center of the bottle, trapping particles inside. However, it is not perfect, as it is limited to particles with a determine velocity and approach angles profiles. Particles outside of that profile, may escape from the bottle.

Another way to approach this problem is by stating adiabatic moment invariance and energy conservation. Adiabatic moment is expressed as:

$$\mu = \frac{mv_{\perp}^2}{2B} \tag{5.2}$$

According to this principle, once that the particle is close to the extreme of the bottle, where the magnetic field is maximum, adiabatic invariance states that the perpendicular velocity reaches a maximum too, leading to a reduction in axial velocity and slowing down the particle. If the particle has great energy (axial velocity), this effect is not high enough to trap the particle, which will then escape.

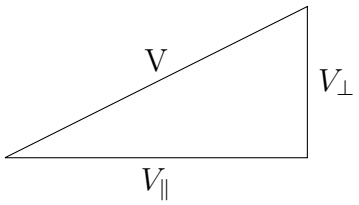

Figure 5.1: Velocity Triangle

From the invariance of the adiabatic moment and considering the velocity triangle, in which we have defined $\sin\theta$ as $\sin\theta = \frac{V_{\perp}}{V_{\parallel}}$ it is possible to obtain the following relationship:

$$\mu = \frac{mv_{\perp}^2}{2B} = \frac{mv^2\sin^2\theta}{2B} = \frac{E\sin^2\theta}{B} = constant \tag{5.3}$$

Bearing in mind that the E, the total kinetic energy remains constant, equation 5.3 states that:

$$\frac{\sin^2\theta}{B} = constant \tag{5.4}$$

Comparing this relation, let's say at the mid plane, where the magnitude of the magnetic field reaches a local minimum and at the position where the magnetic field reaches a maximum yields:

$$\frac{\sin_0^2\theta}{B_0} = \frac{\sin_m^2\theta}{B_m} \tag{5.5}$$

The limiting condition comes when θ reaches a value of 90°. Exceeding that value indicates that the particle will be reflected and, consequently, trapped in the magnetic mirror.

$$\sin_0^2\theta > \frac{B_0}{B_m} \Rightarrow \frac{v_\perp}{v} > \frac{B_0}{B_m} \Rightarrow V_\parallel < v_\perp\sqrt{\frac{B_m}{B_0} - 1} \tag{5.6}$$

This relationship defines a loss cone, that is, a domain in form of cone where the particles with velocities that lay inside that domain will not escape from the magnetic bottle. Particles outside, will escape from the bottle. This cone indicates that particles with velocities almost parallel to the magnetic field lines will experience smaller forces as the angle between their velocity vector and magnetic field would be small, being able to escape.

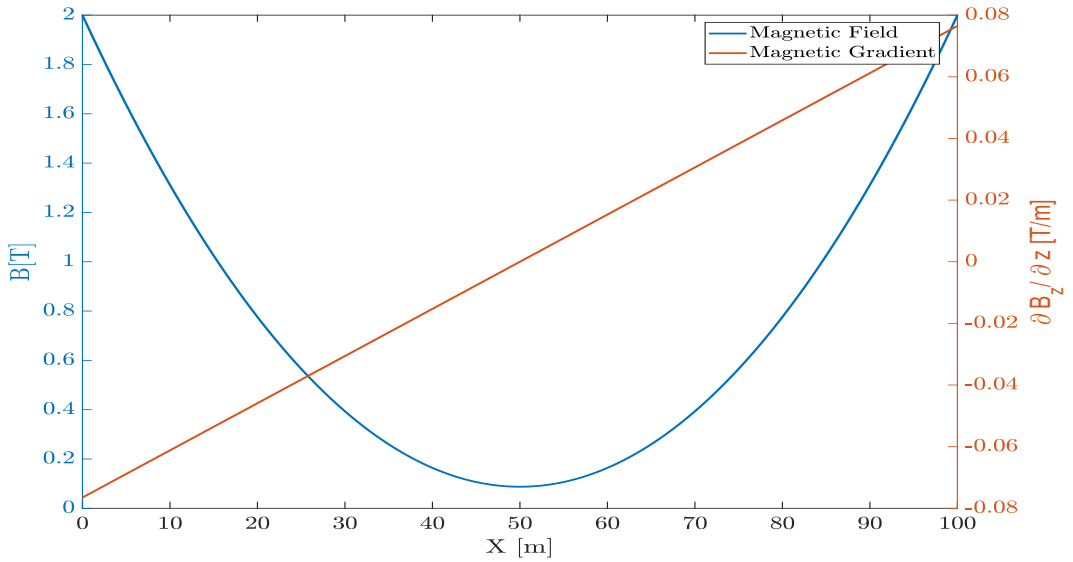

Figure 5.2: Magnetic Field Profile

The represented parabolic profile of the magnetic field has been set for the simulation, being minimum at the center of the domain. Figure 5.2 shows both the profile of the magnetic field and its gradient. It is important that the profile has this or similar shape, otherwise, confinement of charge particles is impossible.

This simulation starts by placing a certain number of electrons at the center of the domain with initial random axial and perpendicular velocities. Then, following the same equations as previously states, the code is run, ending at a sufficiently high time for the particles to show its behaviour, either they are trapped or have escaped. A particle has been considered to escape if at some point of the simulation exists the domain, which in this case has been set to one hundred meters long.

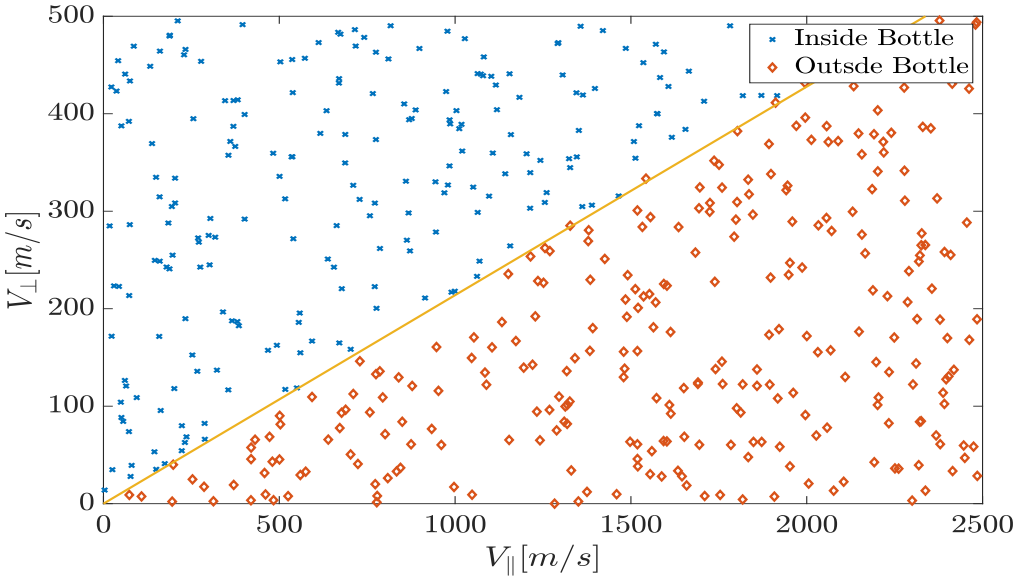

Figure 5.3: Loss Cone

From this Figure it is observed the previously mention loss cone. In yellow, it is appreciated the line that divides the population in particles trapped or escaped. That line represents the relation that 5.6 expresses. Particles below that line are trapped inside the magnetic mirror, otherwise, those particles have enough axial energy to overcome the increasing magnetic field.

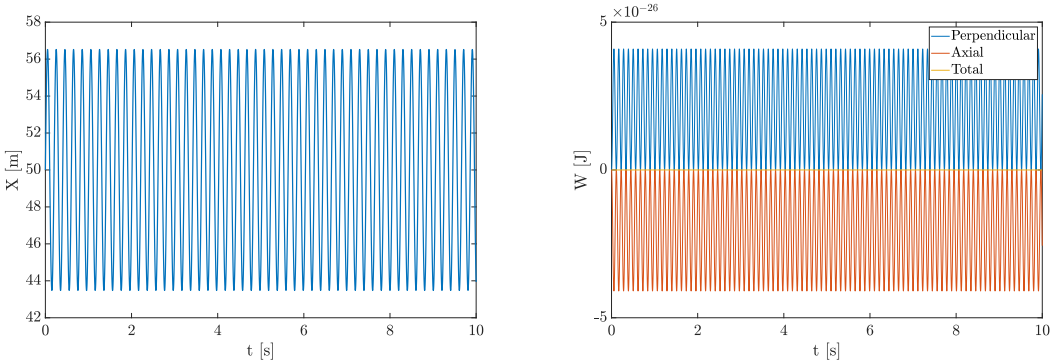

(a) Position

(b) Energy

Figure 5.4: Position and ΔE evolution of a trapped particle

According to the previous Figure, it is observed the net conservation of energy previously stated as there is no gain of energy, only conversion between different velocity components, that lead to an oscillation of the particle inside the domain. As a matter of fact, there is only two possibilities for the particle to escape, being one to gain energy by an external factor such as an electric field or by means of collisions.

As it may be seen, low velocities are considered here for the analysis. For most electron applications, they move at relativistic velocities, far greater that the ones

here. This is done for simulation purposes as greater velocities requires more computational time, however, the explanation stands for different magnetic and velocity profiles.

5.2 Simulation Results

The profile of the RHP wave is obtained by solving Equation 3.20 with the proper selection of plasma properties. Assuming that ω_{pe} and ν_e are independent on the spatial coordinate and assuming a linear decreasing magnetic field, the solution is simplified and can be easily obtained. However as the scope of this project is not based on solving the RHP profile, those were given by the help of the supervisor of this project Álvaro Sánchez Villar. A single scenario is studied here, an underdense case in which the wave faces a population of 10^{15} particles. It will be seen that the wave is able to propagate through the plasma due to the low particle density. In that sense, the wave will be able to propagate at the cost of a decrease in int electric field value, which corresponds to the amount of power deposition. The nature of the encountered plasma severely affects how the wave propagates, being possible the appearance of cutoffs, were the wave is reflected, creating an oscillatory movement in the electric field profile due to the interaction of the incoming wave with the reflected wave. During this simulation, a population of electrons is injected to the domain to analyze the effect of the RHP on the dynamics of those particles. The size of that population is assumed to be sufficiently small so that the plasma properties remain untouched despite those new particles.In that sense, the profile of the RHP remains constant.

For the case of the magnetic profile,it has been selected a linearly decreasing profile, in which the value at the extremes are calculated as follows:

$$B_{zmax} = \frac{B_0}{2} \tag{5.7}$$

$$B_{zmin} = 2(B_0 - B_{zmax}) + B_{zmax} \tag{5.8}$$

where B_0 is the magnetic field at the resonance, which occurs at the center of the domain as the RHP wave indicates. B_0 can be easily computed using the resonance condition:

$$\omega_{ce} = \omega \Rightarrow \frac{eB}{M} = 2.45GHz \cdot 2\pi \Rightarrow B_0 = 0.0876T$$

where the value of the RHP wave frequency has been selected to be 2.45GHz, a microwave frequency used in the MINOTOR project [3]. This particularly set of parameters has been chosen for comparison purposes, as Lieberman, in his book *Principles of Plasma Discharges and Materials Processing* [23], adopts a simplified model of a plasma-wave interaction, allowing for some analytical results.

As the analysis deals with the fact that an electron disturbance is originated at the plasma, some assumptions can be made. First of all, the disturbance is really small compared to the total plasma density, meaning that as a first approximation the electromagnetic forces that arises from this electron distribution is negligible compared to the external applied electromagnetic fields. In addition, the small disturbance does not affect the RHP in a sufficiently high fashion so that it alters its shape.

For this study, an electron population composed of 1500 particles, in which all the population shares the same initial conditions of velocity profile except its phase, which is homogeneously distributed between 0 to 2π, is studied. The parameters that were set for this problem are defined in the following Table.

Initial Parameters	
$V_\perp$	10^5 m/s
$V_\parallel$	$3 \cdot 10^5$ m/s
L	0.6 m
B_{zmax}	0.0438 T
B_{zmax}	0.1313 T
ω	$2.45 \cdot 10^9 \cdot 2\pi$ [rad/s]
ν_e	0.01ω [rad/s]
E_{max}	10 [V/m]

Table 5.1: Initial parameters for the problem setup

5.2.1 Underdense plasma

The underdense simulation scenario is run, where the particle density of 10^{15} m^{-1} has been chosen. Following figure represents the shape of the RHP under the previously explained plasma. As it is seen, for this case the value of the electric field later of the resonance does not reach a zero, meaning that not all the electric energy is absorbed and that the wave is able to propagate through the plasma. For an overdense scenario, the wave would be unable to propagate as the higher plasma density will prevent any further propagation.

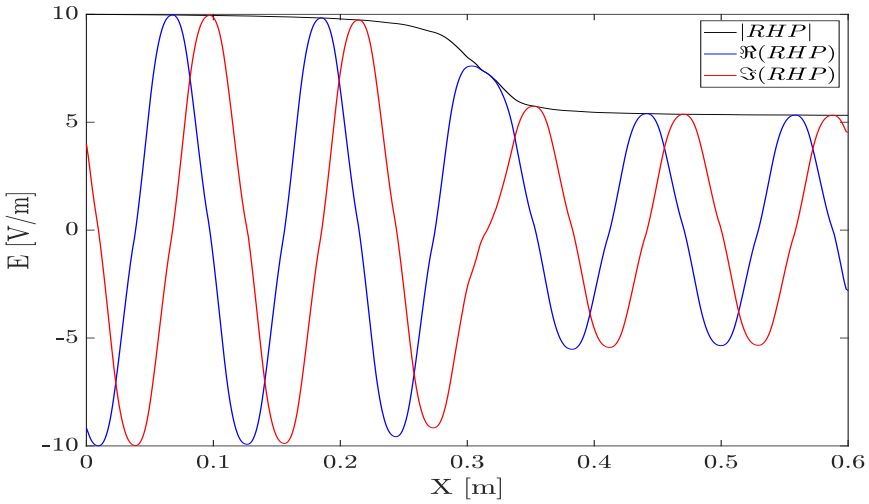

Figure 5.5: Underdense RHP

With all the parameters set, the code can be run, extracting some relevant information for the purposes of this project. Let's start by analyzing the main parameter that defines whether the resonance has taken place or not, the perpendicular velocity evolution. Following figures will plot the evolution of two different particles, one heated by the wave and, thus, gaining perpendicular energy and one that, due to the phase at which enters the resonace, will lose some of its energy.

Starting with the same velocity profile, both particles experience the same initial evolution. The decrease in perpendicular velocity is explained by the magnetic gradient, transforming perpendicular energy into its axial component. As the particles approach to the resonance, oscillations on the perpendicular velocity component starts appearing. This is done because the rate of change of the electron gyrophase equals to the rate of change of the RHP phase at the resonance, and it is there where a sudden jump in perpendicular velocity occurs. Figure 5.6a and 5.6b show this condition.

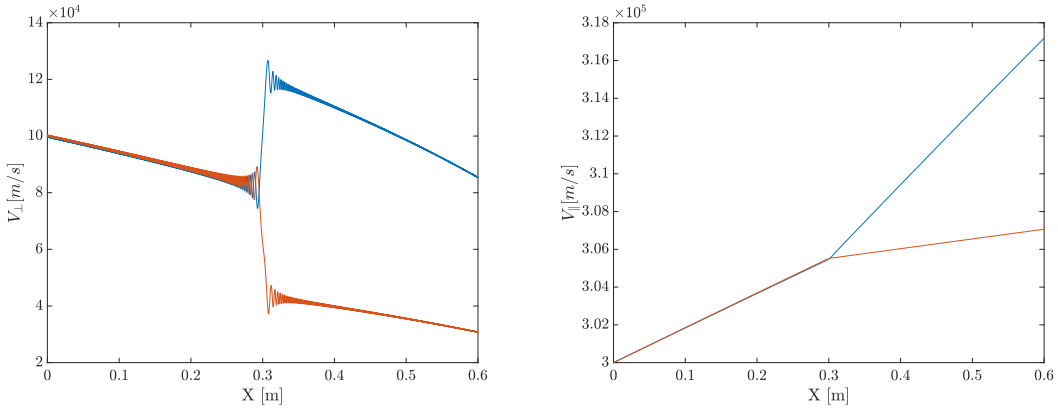

(a) Perpendicular Velocity Evolution

(b) Axial Velocity Evolution

Figure 5.6: Velocity evolution for underdense conditions

For the case of the axial velocity evolution, a great difference is also observed. Once that the particles leave the resonance, due to their new perpendicular velocity, the evolution of their axial velocity component behaves accordingly. As the heated particle has more perpendicular energy to trade, it suffers from larger accelerations, while the particle which has lost some of its energy, suffers from a deceleration. In fact, this behaviour can also be seen at the perpendicular velocity plot, where the particle heated losses at a faster rate its perpendicular velocity.

Notice how the x-axis of the figures represents not the time evolution, but the position of the particle. That is purposely done to make clear where resonance occurs. In this case, it has arbitrarily chosen at the center of the domain.

As part of the study, it is important to check how the parameters affect the heating of the electrons, represented by the increase of the total kinetic energy, defined as the sum of the axial kinetic energy and the perpendicular energy:

$$E_{TOT} = \frac{1}{2} m (v_{\parallel}^2 + v_{\perp}^2) \tag{5.9}$$

According to the Figure 5.7, the net energy gain (or loss) is only due to the resonance. This is something expected since, as previously seen in the magnetic bottle example, magnetic gradients conserve mechanical energy. Previous and after the resonance, no energy changes occur due to the RHP since the evolution of α and β follow different rates

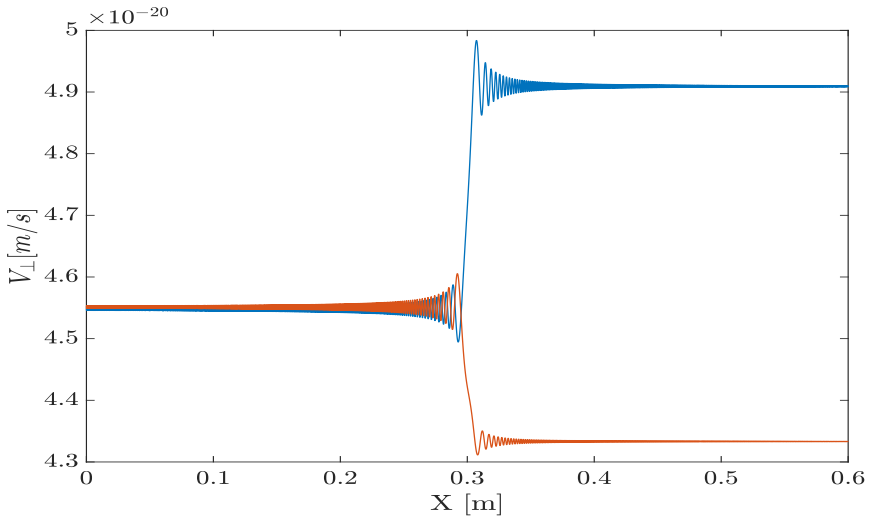

Figure 5.7: Evolution of W_{TOT} for underdense conditions

To make clear how resonance acts on the perpendicular heating, a plot of the evolution of the gyrophase of an electron versus the evolution of the RHP phase is shown in Figure 5.8.

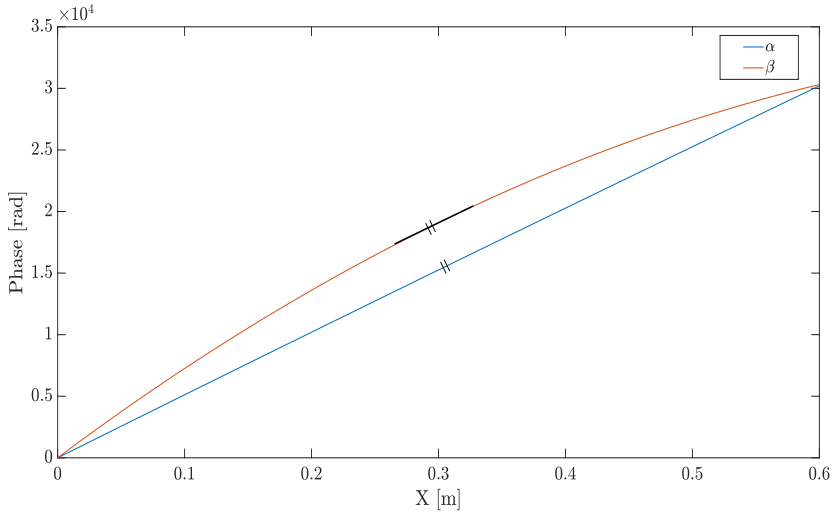

Figure 5.8: Phase comparison: α *and* β

It is highlighted in the former figure how the rate of change of the electron phase is nearly equal to the angular rotation of the RHP at the resonance. It is said nearly because of the second term of the expression 4.16, which will act whenever there is a difference between phases. As a simple order of magnitude will show, this term does not drive the evolution of the electron's phase but, at the resonance, acts as a way to reduce the difference between α and β. For the case in which, at the resonance position, the phase difference is exactly zero, the rate of change for both is exactly equal since that second term vanishes and, due to the proper selection on the magnetic field, β evolves at the same rate than α.

For comparison reasons with Liebermann, this underdense case is selected to validate the obtained results. In his book, Liebermann [23] develops a analytic expression for the change in perpendicular velocity that a single electron experiences as it passes through the resonance. Assuming a stationary phase method, the increment in velocity can be expressed as:

$$\Delta A = -\frac{eE_{res}}{m_e}\sqrt{\frac{\pi}{\omega\alpha v_z}}(1+i) \tag{5.10}$$

where E_{res} is the electric field at the resonance, v_z is the axial velocity at the resonance and α is a value representing how the magnetic field changes across the domain:

$$\alpha = \left|\frac{1}{B_{res}}\frac{dB}{dz}\right| \tag{5.11}$$

Notice how the change in velocity is expressed as a complex number, expressing the perpendicular plane as a complex plane. Foremost, only the velocity of the electron

appears on the expression, stating that the change in velocity does not depend on the initial phase of the electron but on its axial velocity. However, despite the fact that the change in velocity is independent of the initial phase, due to the initial position of the perpendicular velocity on the complex plane, some phases will experience a greater heating. Averaging the initial gyrophase of the electron distribution, the mean mechanical energy gained by an electron can be derived as follows:

$$W_{ecr} = \frac{1}{2} m_e \Delta A \cdot \Delta A^* = \frac{\pi e^2 E_{res}^2}{\omega \alpha v_z m_e} \tag{5.12}$$

where superscript * represents multiplication by the complex conjugate. This analytical result will be helpful for comparison purposes as some parameters will be tuned to check how they affect the net mechanical energy gained.

The implication of Expression 5.10 can be seen by drawing what is the change in perpendicular velocity of an electron population whose initial perpendicular velocity is the same, with its phase distributed homogeneously from 0 to 2π. As the change in velocity is independent of the phase of the velocity, all electrons will experience the same change in velocity in the perpendicular plane, but due to the individual electron phase, some of the suffers a greater difference form its original velocity.

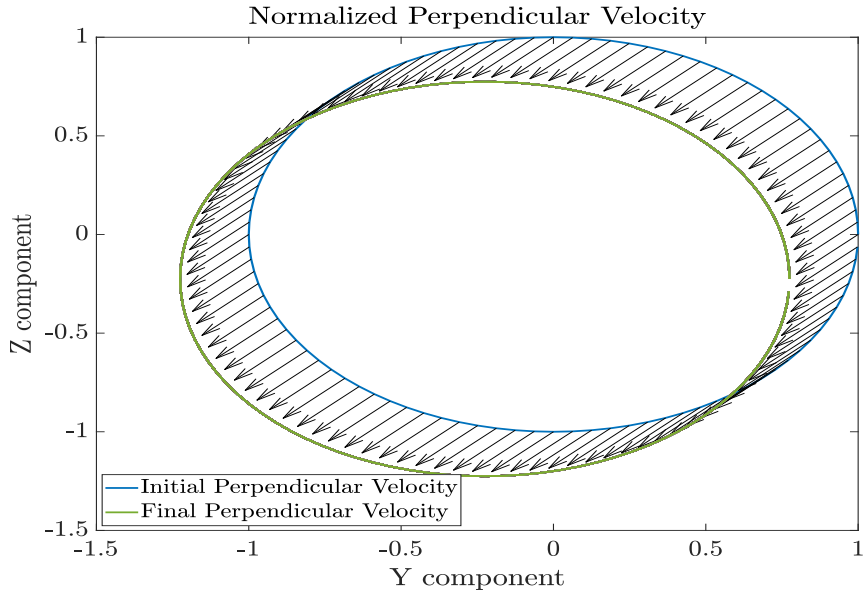

Figure 5.9: Change in the perpendicular velocity for a population of electrons with same perpendicular velocity but different phase

This effect is observed in Figure 5.9. The global effect of the RHP on the plasma, is a net heating of the electrons that composed the plasma. However, certain phases are preferred in terms of plasma-wave interaction. It is possible also that some groups of electrons lose energy as its final perpendicular velocity results in a lower value than the initial one.

As the variation in velocity due to the magnetic nozzle is that so the total energy is conserved, the total increment in energy is created by the interaction between the plasma and the wave. A proper selection of parameters is key on the performance of ECR thruster. In this simulation, it has been defined a mean mechanical energy. This definition is interesting as not all the electrons heats evenly. Due to the initial phase condition, some electrons experience greater heating, gaining more energy in the process. It is possible even that some electrons lose energy as the perpendicular velocity vector and the RHP wave vector may point in different directions. For the initial parameters selected, the mean mechanical energy gained per electron is:

$$W_{simulation} = 1.131 \cdot 10^{-21} J;\ W_{analytical} = 7.218 \cdot 10^{-22} J$$

a) Change in initial axial velocity

For the computation of the analytical expression, special care has been taken while considering the axial velocity as, due to the magnetic gradient, it evolves from the given initial value up to the resonance one.

$V_{\parallel}$ [m/s]	$W_{simulation}$ [J]	$W_{analytical}$ [J]
$3 \cdot 10^6$	$9.245 \cdot 10^{-23}$	$7.218 \cdot 10^{-23}$
$3 \cdot 10^4$	$1.124 \cdot 10^{-22}$	$7.218 \cdot 10^{-21}$
$3 \cdot 10^3$	$9.147 \cdot 10^{-20}$	$7.218 \cdot 10^{-20}$

Table 5.2: Axial velocity effect on mean mechanical energy

The total gain in mechanical energy is influenced by the axial velocity of the particles. The reason behind this behaviour is the residence time at the resonance zone. A characteristic resonance time can be estimated as $t = \frac{L_r}{v_{axial}}$, where L_r is defined as the resonance length. The more time an electron resonates with the RHP wave, the greater its increase in total energy, since when resonance occurs, the electron sees a static electric field.

b) Change in initial perpendicular velocity

$V_{\perp}$ [m/s]	$W_{simulation}$ [J]	$W_{analytical}$ [J]
10^6	$8.954 \cdot 10^{-22}$	$7.218 \cdot 10^{-22}$
10^4	$1.145 \cdot 10^{-21}$	$7.218 \cdot 10^{-22}$
10^3	$9.146 \cdot 10^{-22}$	$7.218 \cdot 10^{-22}$

Table 5.3: Perpendicular velocity effect on mean mechanical energy

No significant change in the mean mechanical energy is observed as the initial perpendicular velocity is tuned. The difference in the values are surely due to the numerical solver employed. The effect on varying the perpendicular velocity is purely changing the value of the Larmor radius but no effect in the plasma-wave interaction.

c) Change in total domain length

Length [m]	$W_{simulation}$ [J]	$W_{analytical}$ [J]	α $[m^{-1}]$
10	$2.17 \cdot 10^{-20}$	$1.203 \cdot 10^{-20}$	0.1
1	$3.35 \cdot 10^{-21}$	$1.203 \cdot 10^{-21}$	1
0.1	$4.82 \cdot 10^{-22}$	$1.203 \cdot 10^{-22}$	10

Table 5.4: Domain length effect on mean mechanical energy

Table 5.4 shows that increasing the total length of the domain leads to an increase of the total energy gained. As the extreme values of the magnetic field remain untouched, the increment in length decreases the magnetic gradient along the main axis. According to Gammino [24], a lower magnetic gradient leads to a wider resonance zone, where electrons are able to gain more energy. As a side effect as well, although less important, as the magnetic gradient decreases, the energy conversion from perpendicular to parallel due to the magnetic nozzle is carried is a slower pace, s at the time of resonance, the axial velocity is lower, spending more time at the resonance.

d) Change in E_{res} of the RHP

For simplicity, the value of E_{res} has been taken as the value of the electric field at the center of the domain, where the resonance is imposed. However, the computation of this value is not trivial. Several aspect affect this value, in which the Doppler effect can be found. Due to the difference in velocity between the wave and the electrons, the value of E_{res} is shifted by a certain value. Special care must be taken.

E_{res} [V/m]	$W_{simulation}$ [J]	$W_{analytical}$
25	$5.248 \cdot 10^{-20}$	$7.021 \cdot 10^{-20}$
7	$4.734 \cdot 10^{-21}$	$5.504 \cdot 10^{-21}$
0.5	$3.987 \cdot 10^{-23}$	$2.816 \cdot 10^{-23}$

Table 5.5: RHP wave effect on mean mechanical energy

It is seen that the greater the value in the electric field of the RHP wave at the resonance, the greater the energy gained. This is due because that value represents the amount of power that electrons absorb from the wave. Nevertheless, the reader must bear in mind that that wave represents perfect power absorption. In real engines,

that absorption is highly dependant on the amount of power used to generate the microwave and plasma properties. For instance, a high density plasma may avoid wave penetration, causing what it is called a cutoff.

The variation of this parameters shows interesting results in the amount of heating an electron population is subjected to. Firstly, the amount of power that is transmitted to the plasma is given by the electric field at the resonance. However, higher values of the electric field, not only imposes more restrictions in terms of power input but it may lead to instabilities or cutoffs.

Secondly, in this model, the lower the magnetic gradient, the greater the net heating of the electron population, reaching a limit at null gradient. Finally the residence time of the electrons at the resonance region highly affects the perpendicular acceleration of the electrons. Theoretically, a static electron will heat indefinitely until relativistic effects are important. However, as that electron has no axial velocity component, cannot be accelerated by the magnetic nozzle.

An interesting fact that arises from interpretation of Figure 5.9 is the fact that the resonance tends to gather the different gyrophases into a unique value. This can be seen by how the circle is squeezed after the population has passed through the resonance. The physical explanation is that the wave, at the resonance, tends to synchronize the different phases with its own phase, forcing the electrons to rotate at the same phase as the RHP.

This behaviour can be seen in the following Figure, where the evolution of the phase at different instants of time is represented in an histogram plot.

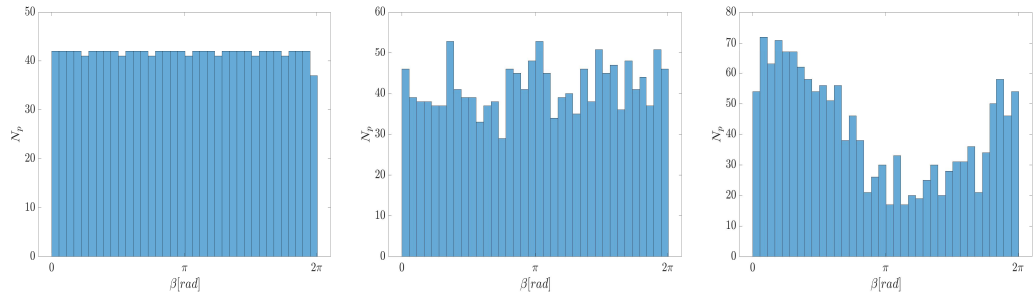

(a) (b) (c)

Figure 5.10: Evolution of the electron phase

Starting the simulation with an homogeneously distributed electron population, the profile of the different histograms changes and the phase evolution follows the evolution dictated by the set of ordinary differential equations that describes this problem. As the particles intersect the resonance, its phases evolve in a noisy way. No interpretation results here. However, as the particles exit the resonance, a peak in the number of particles that shares a common phase it is visible, as already explained,

showing how the effect of the RHP forces the electrons to accommodate its phase with the rotation of the electromagnetic wave.

As a final test of showing how the polarized wave affects the phase of the electron, a simulation is run, in which the magnetic gradient is tuned to be zero, setting a value for the field of B_0 , the resonance magnetic field. During this simulation, a small sample of electrons is studied as the general behaviour will remain untouched. According to the set magnetic field, all electrons start the simulation at the resonance condition, being that constant along the domain as no change in the field is experienced.

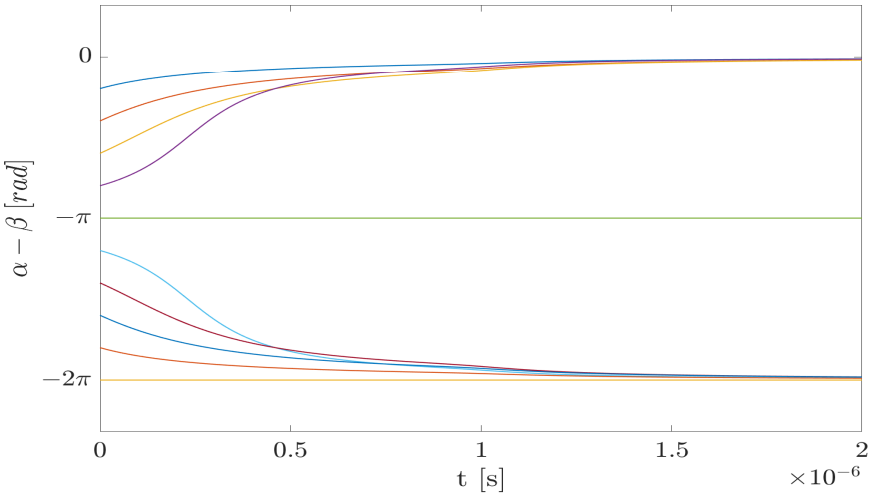

Figure 5.11: $\alpha - \beta$ *evolution*

As the previous Figure shows, in a full resonance, as the particles evolve, the difference between the phases is continuously reduced until reaching a null difference (o or 2π), stating that the particle is being heated at all instants of time, except for the particle whose difference in phase is π. Due to the condition set by the set of differential equations, that particle will lose energy until reaching a zero perpendicular energy. At that point, the particle will be heated again. That electron is said to be at an unstable equilibrium. Any action that alters its phase, such a collision, will lead to a null difference.

Although this setting seems the best option regarding the heating of the particles, building such mechanism results unfeasible for several reasons. Firstly, the resonance should be located inside certain boundaries for engine manufacturing. Secondly, achieving a constant magnetic profile is impossible as the divergence of the magnetic field is zero, stating that, the further from the magnet or solenoid, the lower its intensity.

A clear indication to observe how some electrons suffers from greater accelerations is to assume that the electron disturbance follows a Gaussian distribution in which all the particles inside has the same initial velocities but different initial phases. If

all the electrons are heated evenly, it is expected that the initial Gaussian distribution is kept constant as time passes. However, due to the natural behaviour of resonance, this distribution spreads out as more and more electrons resonate, the initial distribution disappears .

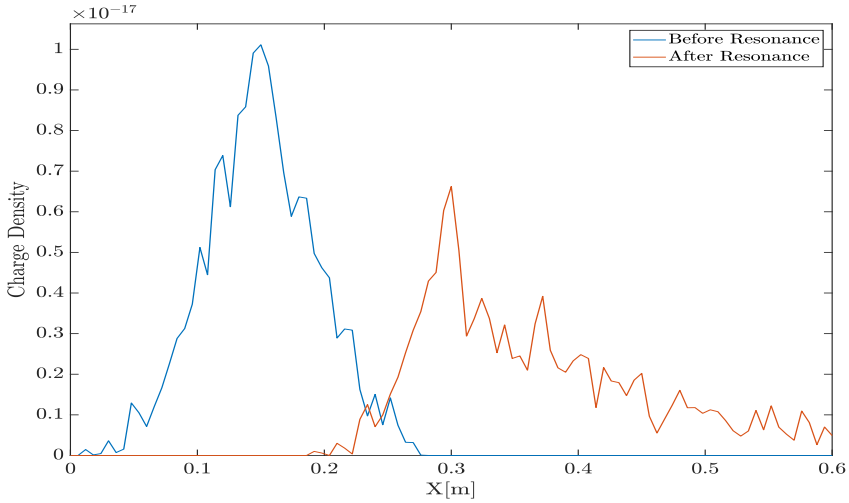

Figure 5.12: Charge density [C/m] along the domain [m]

As a validation of the PIC weighting system, the are below the curve of the charge density represents the total charge of the electron distribution, and thus, the net amount of particles that made up the disturbance. That charge, without the injection of external particles remains constant over time, except when particles leave the domain. Figure 5.13 shows this evolution. Despite the fact that some electrons are experiencing grater accelerations, the area under the curve is kept constant.

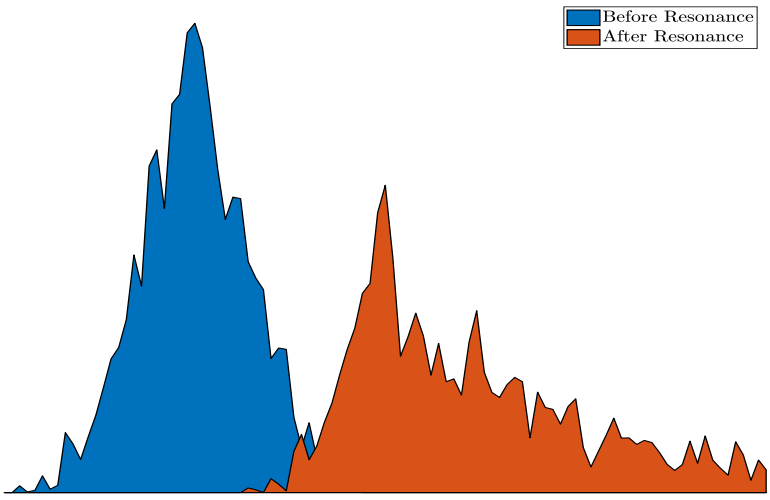

Figure 5.13: Net amount of charge inside the domain

For a typical charge distribution, the net amount of charge is computed by means of an integral as:

$$Charge = \int_a^b \rho(x)dx \tag{5.13}$$

where a and b represents the limits of the domain where the total charge is computed. However, considering the PIC model, where space is discretized, the integral form is reduced to a sum of the discrete values of the charge density distribution. For the computation of the total number of particles, as only electrons are considered for this analysis, dividing the total charge by the elementary charge value yields the net amount of particles.

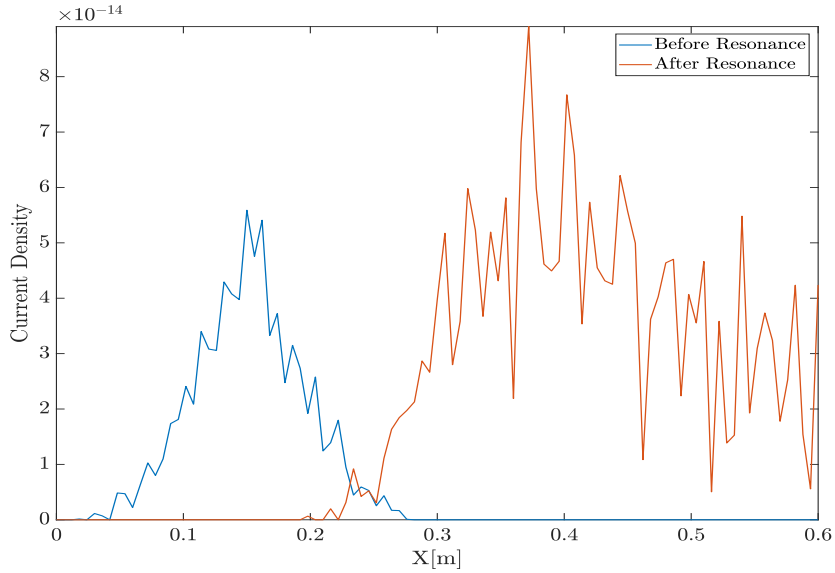

Figure 5.14: Current density [C/s] along the domain [m]

Figure 5.14 shows the evolution of the current density of the electron distribution. It starts with the initial Gaussian distribution and it evolves in time, changing its value. As the particles are accelerated, the current density, a measure of how many charges passes through a certain point, increases.

The lack of smoothness in the graphs is due to the low computational power of the computer employed. For more accuracy, more particles and smaller grid cells should be employed. However, due to the limitations with the current technology, this is the maximum accuracy possible. Recall that the set of equations are being solved by each individual particle. This results in larger computational times and memory usage which, unfortunately, the computer cannot handle.

With the introduction of a Gaussian distribution, the effect of the self-induce electric field created by the electrons' position can be studied and checked. For this particular simulation the boundary conditions of the potential have been chosen to be zero

to showcase the small induced electric field of the particles. The following figure shows the electric field created by the population at the beginning of the simulation

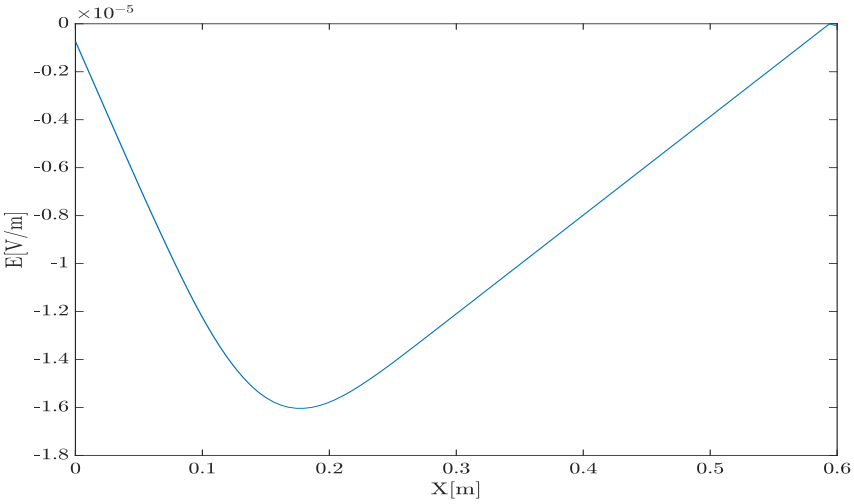

Figure 5.15: Electric Field due to the position of the charges

Notice how in this Figure 5.15 the electric field reaches a peak where the concentration of electrons is maximum. as the charge density is greater. Then, the graph evolves to satisfy the boundary conditions. The value of the electric field, although included in the dynamics of the electrons, does not affect their movement in a sensible way, as the main driver for the axial movement is due to the magnetic gradient.

$$\frac{eB}{m_e} \sim O(10^{10}) \; ; \; \frac{v_\perp^2}{2B_z}\frac{\partial B_z}{\partial z} \sim O(10^{12})$$

This limited number of particles that has been place for the setup of the simulation is purposely done for physical consistency as the shape of the RHP is assumed to be constant and large population of charge particles would alter the profile. Although included in the simulation, the electric forces play little role on the particle movement. For different simulations, a greater number of particles may be chosen, according the the specified problem. Recall that a feat of PIC codes is the ability of introducing macro-particles, a cloud of elemental particles that can be simulated as a whole, speeding up the computational process.

Conclusions and future work

During the past few decades, electric propulsion has interrupted in the propulsive market with really good performance. Its reduction on fuel cost due to the high specific impulse they provide and its great control in stability performance make them perfect for orbital keeping manoeuvres. However, some problems must be addressed to completely depend on this technology, such as power performance and its limited lifetime. In that sense, electrodeless engines are being studied. Those engines eliminate the use of a neutralizer, an electrode whose erosion limits the lifetime of the well-known electric engines such as the Gridded Ion Thruster.

One of the principal electrodeless engines is the one studied during this project, the Electron Cyclotron Resonance thusters. These engines are based on the principle of plasma-wave interaction, in which a microwave heats an electron population while a magnetic nozzle accelerates them. A simplified code detailing the evolution of those electrons has been developed to study this plasma-interaction. By analyzing the results of the code, it has been observed how the heating of an electron is produced and some results have been obtained.

The code solves for the evolution of the parallel and perpendicular velocities and the phase evolution of each electron as well. Some results were expected such as its axial acceleration due to the magnetic nozzle or the increase in perpendicular energy due to the resonance while some others like the coalescence of the phases due to the effect of the wave. It is also important to remark the contribution of PIC codes to the general studies in plasma. Its ability to mesh particle properties on a grid and how they are able to deal with macro-particles make them perfect for custom codes in the majority of possible scenarios.

An underdense scenario where the wave is able to propagate thought the plasma has been studied. This case has thrown some significant results in terms of net heating. Large electric fields, lower magnetic gradients and greater resonance times are some of the characteristics that affect the total heating of the electrons.

The study of ECR thrusters is only at its beginnings. Although its first appearance on experiments and papers was more than fifty years ago, due to the limitations at the time of researching them and the absence of great power units let investigations to a dead end. Only during the past two decades, significant advances were made by different investigation groups, whose task has been recognized by the international institutions.

6.1 Future work

In this project we have developed a program that moves electrons under the presence of a given RHP wave and weights its properties on a 1D mesh grid. This allows for a first understanding of the plasma-wave interaction, how the electrons resonates with the polarized wave. However, the profile of the microwave does not represent a self-consistent solution of the problem although it has been investigated the effect of a wave in a small population of electrons.

For a future work, different plasma densities and initial conditions may be studied, as well as what are the optimal parameters that will result in higher accelerations. In that sense, the electromagnetic forces created by the movement of particles may not be negligible. For instance, an interesting simulation would consist in accelerating electrons and see how the ions are accelerated due to the absence of negative charges.

As an addition, a future code will include the fact that the RHP depends on the plasma properties, that is, for a given initial condition, the microwave is extracted. Positions and velocities of particles are updated at each time step, changing how the wave behaves. In that sense, cold plasma approximation must be discarded as finite inhomogeneous plasmas do not accept this simplification. Following Figure details the loop for a self-consistent solution of this kind of problem

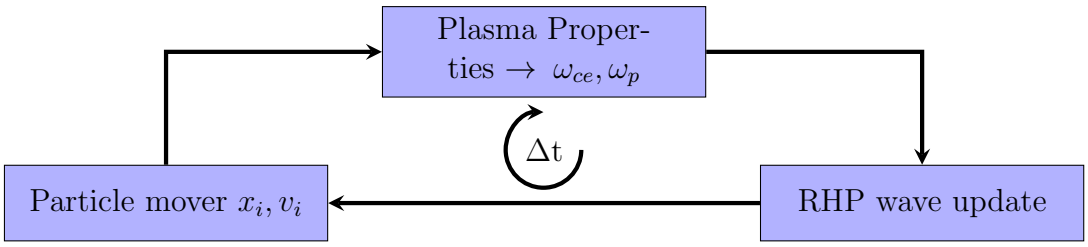

Figure 6.1: Logical loop of a self-consistent solution of a RHP wave-plasma interaction

Appendix

Appendix A

Budget Analysis

As part of this project, a budget analysis has been done, reflecting the amount of money this project would have cost in the actual market. Different factors should be taken into account while making this analysis, such as the total component cost or the software price.

Budget Analysis	
Salaries	3240
Alumni	3240
Cost equipment	220.22
Depreciation	16.22
Windows 10	135
Matlab Software	69
Total	3440.22

- Salaries

For the alumni salary, it has been assumed a net work of 360 hours divided in a period of 9 weeks, as recognized by the 12 ECTS that the bachelor thesis is based on. According to the salary of a recent graduate publish by the **Boletín Oficial del Estado** [25]

$$Salary\ Alumni = 360 hours \times 9\ €/\text{hour} = 3240\ €$$

- Equipment Cost

In the equipment cost, the price of the computer as well as its depreciation, alongside the Matlab license it is included. Regarding the cost of the computer, the model used during the whole process of the project is valued around 750 euros. Assuming a linear depreciation and considering that the useful life of a typical home laptop is around 8 years, the total cost due to depreciation results in:

$$Depreciation\ Cost = \frac{750€}{8\ years \times 52\ weeks} \times 9\ weeks = 16.22€$$

Regarding the cost of the operational software, Matlab offers annual licenses at the price of €800 as well as perpetual license of €2000 . Due to the length of the project, an annual license is considered. However, Matlab includes an student version of its software, which use is restricted to educational purposes on academic institutes at the price of €69. This last option is the one that has been selected.

Finally, the operational system in which the computer is based on. For this particular case, Windows 10 was the one which has been used. By simply taking a look at the actual price of this system, a total of €135 would have been invested.

Bibliography

[1] ESA. Funding.

[2] Kamesh Sankaran, Luigi Martinelli, and Edgar Choueiri. A flux-limited numerical method for the mhd equations to simulate propulsive plasma flows. 06 2000.

[3] Julien Jarrige, Paul-Quentin Elias, Félix Cannat, and Denis Packan. *Performance Comparison of an ECR Plasma Thruster using Argon and Xenon as Propellant Gas*. 2013.

[4] Justin M. Little. *Performance Scaling of Magnetic Nozzles for Electric and Propulsion*. 2015.

[5] C. K. Birdsall A. B. Langdom. *Plasma Physics and via Computer and Simulation*. Adam Hilger, 1991.

[6] D Packan, PQ Elias, J Jarrige, M Merino, A Sánchez-Villar, E Ahedo, G Peyresoubes, K Holste, P Klar, M Bekemans, et al. *The MINOTOR H2020 project for ECR thruster development*. 2017.

[7] Kimberly Amadeo. How $ 1 spent on nasa adds $ 10 to the economy.

[8] Paul G Dembling and Daniel M Arons. The evolution of the outer space treaty. 1967.

[9] Filippo Cichoki. *Analysis of the expansion of a plasma thruster plume into vacuum*. 2017.

[10] Robert J Goldston and Paul Harding Rutherford. *Introduction to plasma physics*. CRC Press, 1995.

[11] NASA. NASA's evolutionary xenon thruster-commercial (NEXT-C).

[12] Goebel Dan M and Ira Katz. *Fundamentals of Electric Propulsion: Ion and Hall Thrusters*.

[13] Jaume Navarro-Cavallé, Eduardo Ahedo, Mario Merino, Vıctor Gómez, Mercedes Ruiz, and José Antonio Gonzalez del Amo. *Helicon Plasma Thrusters: prototypes and advances on modeling*. 2013.

[14] Joel C. Sercel. *Electron-Cyclotron-Resonance (ECR) and Plasma Acceleration*. 1987.

[15] *An Experimental and Theoretical Study of the ECR Plasma Engine*. 1993.

[16] HG Kosmahl. Three-dimensional plasma acceleration through axisymmetric diverging magnetic fields based on dipole moment approximation. 1967.

[17] Hiroshi Matsumoto and Yoshiharu Omura. *Particle Simulation of Electromagnetic Waves and Its Application to Space Plasmas*. Springer Netherlands, 1985.

[18] Mario Merino, Álvaro Sánchez-Villar, Eduardo Ahedo, Paul Bonoli, Jungpyo Lee, Abhay Ram, and John Wright. *Wave Propagation and Absorption in ECR Plasma Thrusters*. 2017.

[19] Kimitaka Itoh Akira Yoshizawa, Sanae-I Itoh. *Plasma and Fluid Turbulence: Theory and Modelling*. Plasma Physics.

[20] Yoshiharu Omura. *One-dimensional Electromagnetic and Particle Code: KEMPO1*. 2007.

[21] T.Zh. Esirkepov. *Exact charge conservation scheme for Particle-in-Cell simulation with an arbitrary form-factor*, volume 135. 2001.

[22] Viktor K. Decyk. *Description of Electromagnetic Spectral Particle-in-Cell Code from the UPIC Framework*.

[23] Michael A. Lieberman and Allan J. Lichtenberg. *Principles of Plasma Discharges and Materials Processing*.

[24] S Gammino, D Mascali, L Celona, F Maimone, and G Ciavola. *Considerations on the role of the magnetic field gradient in ECR ion sources and build-up of hot electron component*, volume 18. IOP Publishing, 2009.

[25] BOE. Boletin oficial del estado num 45 sec III otras disposiciones, February 2018.